UCRL-51352

THE PHYSICS OF SOC AND TENSOR

John F. Schatz

February 21, 1973

Prepared for U.S. Atomic Energy Commission under contract No. W-7405-Eng-48

LAWRENCE
LIVERMORE
LABORATORY
University of California/Livermore

Printed in the United States of America
Available from
National Technical Information Service
U. S. Department of Commerce
5285 Port Royal Road
Springfield, Virginia 22151
Price: Printed Copy $___*; Microfiche $0.95

*Pages	NTIS Selling Price
1-50	$4.00
51-150	$5.45
151-325	$7.60
326-500	$10.60
501-1000	$13.60

TID-4500, UC-35
Nuclear Explosives—
Peaceful Applications

LAWRENCE LIVERMORE LABORATORY
University of California/Livermore, California/94550

UCRL-51352

THE PHYSICS OF SOC AND TENSOR

John F. Schatz

MS. date: February 21, 1973

Contents

THE PHYSICS OF SOC AND TENSOR

Abstract

SOC and TENSOR (respectively, one and two dimensional finite difference computer codes for the calculation of stress wave propagation) are described in some detail from a physical viewpoint. Emphasis is placed on the treatment of constitutive relations (equations of state) as this is the facet of the calculational method which most often causes difficulties. It is shown that not all of the models are entirely physically or numerically plausible, but that they are often adequate if understood and manipulated properly. Several sample calculations are presented.

It is concluded that SOC and TENSOR require extensive revision. To this end, a new one-dimensional code, called SOC73, has been developed, and an improved two-dimensional code is being formulated.

Introduction

This report is an elementary description of the physical reasoning and method contained in two finite-difference, artificial viscosity method computer codes (programs) which have been developed at the Lawrence Livermore Laboratory. The two codes, called SOC and TENSOR, are intended for the Lagrangian calculation of time-dependent initial value problems involving, respectively, one and two dimensional adiabatic motion of a medium. Both codes were developed primarily for computing the geophysical effects of nuclear explosions.

Explosion-caused motion generally results in a shock wave, or a rapid, very nearly discontinuous increase in pressure which propagates through the material. The shock wave eventually decays into an elastic wave. SOC and TENSOR are different from the so-called hydro codes in that they heavily emphasize the complicated stress-strain response of the rock medium and therefore do not generally assume that the medium acts as a fluid, or even nearly as a fluid.

SOC and TENSOR are now written, so far as possible, so that they contain the same physics in one and two dimensions, respectively. Here, we intend to describe the physics of the codes in a way that the user can more readily comprehend the built-in models of material behavior and obtain an understanding of the interrelationship of parameters, calculations, and results. We will be operating under the assumption that the details of logic and numerical methods are correct and of sufficient power to deal with the problems at hand. Much of the essential mathematics and some of the physics are documented for

SOC by Seidl[1] and Cherry and Petersen[2] and for TENSOR by Maenchen and Sack[3] and Cherry, Sack, Maenchen, and Kransky,[4] but reference to these documents is not prerequisite to the understanding of this report.

In association with the term motion one sees the terms stress wave and strain wave. If the infinitesimal elements or particles of a medium have any effect upon one another, then the forced motion of one or a group of particles at any point or points will eventually be transmitted, though possibly in some distorted fashion, to the remainder of the medium. Wave-like motion is often termed a stress wave when the mechanism of transmittal of energy is the stress, or force acting upon particles of the medium. However, because we usually observe in the field or laboratory the displacements, or strain of the medium, a term which often appears is strain wave. (Strain refers to any relative displacement which cannot be described as a rigid body displacement of the entire medium.) For most purposes, the terms stress wave and strain wave are interchangeable. If a particle is strained, but, upon the release of the stress causing the strain, the particle returns to its original configuration, then the medium is deemed elastic. If stress is linearly related to strain, then the term linear elastic is used, though writers have begun to use several terms interchangeably to describe linear elasticity, e.g., perfectly elastic, Hookean, simple elasticity, or just "elastic." We will use the terms elastic and linear elastic as defined above, and we will refer to any departure from elasticity as non-elasticity.

An adiabatic process is one in which the system under consideration (in our case the particle) is thermally isolated from its surroundings. For a time dependent process, thermal isolation must continue for a time comparable to the time scale of the process. Explosion-produced shock fronts are generally transmitted through the entire medium of interest in a few milliseconds, and slow-moving seismic wave fronts are transmitted in times not longer than a few seconds. The time scale of normal heat transfer processes in a medium consisting of solid geologic materials is minutes or more. Therefore, normal heat transfer simply does not have an effect on the mechanical transfer of energy in the wave, and we assume adiabaticity. An exception occurs at very high temperatures where radiative heat transfer (which is essentially instantaneous) is important. However, we are usually not quantitatively interested in calculations as near to the source of energy where the temperature would be so high. The adiabatic assumption has two main effects on the calculations. The first is that thermal parameters such as thermal conductivity and heat capacity do not have to be taken into account. The second is that the energy deposited in the medium by the wave motion is only that mechanical energy introduced by the compression, distortion, and acceleration of the material.

The calculational method used by SOC and TENSOR is called the finite difference method. It will not be described here; however, the following general considerations are of interest. If the problems to be solved are assumed to

be governed by a set of sufficiently general partial differential equations, then the essence of the finite difference approach is that the derivative $\partial f(x)/\partial x$ may be replaced by $f(x_1)-f(x_2)/x_1-x_2 = \Delta f/\Delta x$ for small but finite values of both numerator and denominator. Here f(x) is any function of a generalized variable x (which may be space or time). In other words, the infinitesimal increments into which the medium is divided in order to treat it as a continuum are now considered to be increments of a small but finite size. Such a finite increment in space for us is called a zone, and in time is called a time step.

In order for a calculation to be physically realistic, the properties of the medium must be continuous over dimensions comparable to the finite Δx. The discontinuities which arise in shock waves are taken care of by calculational ploys such as artificial viscosity, which smear a shock over several Δx's in order to minimize the discontinuity, but still allow a sudden enough onset to approximate the real-world shock.[5] There are, unfortunately, many other pitfalls of discontinuity which must be avoided, several of which will be discussed later. If discontinuities must occur, they should be accompanied by the use of appropriate boundary conditions to patch up the otherwise inherent breakdown of the finite difference method. Also, the physical equations cannot be allowed to depend directly on the zone or time step size, because the zone is an approximation of an infinitesimal volume and as such has no physical reality.

When motion of a medium is discussed, one must have some way of describing that motion which is well-suited to the problem. Let us say that we wish to describe the velocity of the medium as a function of time. There are two common ways. We can "follow" a mass particle and describe its velocity as a function of time, or we can establish a fixed point in the medium, and describe the velocity at that point (many particles may move by) as a function of time. The former description, that of "following" an element is called Lagrangian and the latter Eulerian. The Eulerian description is particularly suitable when one is interested in identifying particle path lines, or making sense out of pictures of flow, while the Lagrangian description, which follows particles of constant mass, is easy to adapt to the finite difference technique. The Lagrangian particles become simply the finite zones of the problem. The zones are allowed to move and distort with the material, but the mass within them is not permitted to flow in or out.

It should be made clear before we enter into detailed description that several of the assumed aspects of material behavior contained in SOC and TENSOR are neither well-founded nor generally agreed upon in the scientific or engineering communities. Calculations in which these questionable aspects arise may lead the user to erroneous conclusions. Nevertheless, the evidence of past calculations indicates that the codes are usually adequate, provided that the user is experienced, and that he has access to a set of correct and sufficient input data.

A Simple Description of the Physics of SOC and TENSOR

To begin with, one imagines a one or two dimensional cross section of the medium (usually a geologic cross section) for the problem he is interested in solving. For example, a SOC problem might be to initiate ground motion by pressure as a function of time acting on a spherical cavity (Fig. 1). Then the motion propagates to a free surface in spherical symmetry and returns by reflection. A TENSOR problem might be similar except that the volume is divided into several plane layers and bounded by a plane free surface in cylindrical symmetry (Fig. 2). Several other symmetries, configurations, sources, and boundaries are available.

Once one has the general configuration in mind, he may assign different materials (e.g., gas, Rock Type I, Rock Type II, etc.) to different regions; then

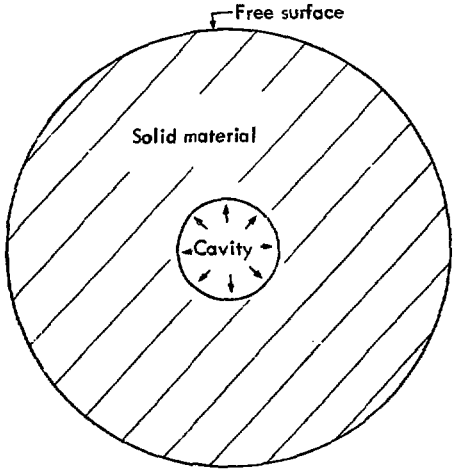

Fig. 1. Configuration of a typical SOC problem. Others are possible.

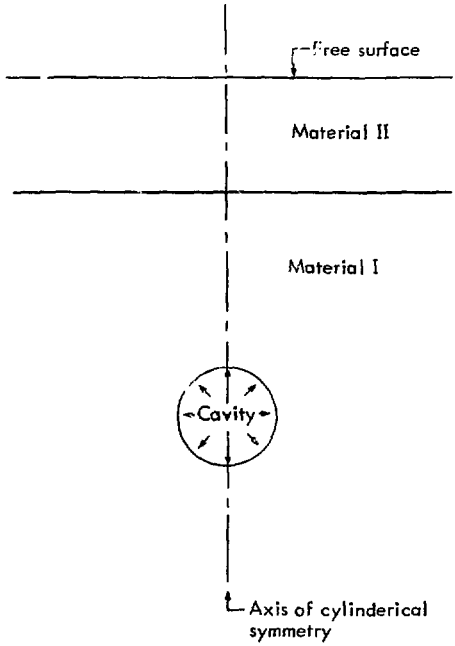

Fig. 2. Configuration of a typical TENSOR problem. Others are possible.

he divides the entire problem up into the small zones which will be manipulated by the finite difference equations. (A region in general contains many zones.) In SOC, the available symmetries are plane and spherical, and in TENSOR they are plane and cylindrical. In SOC, interior boundaries cannot slip (one dimensionality forces this) or separate from one another (an arbitrary restriction to simplify coding). Exterior boundaries may be either free or rigid or determined by a specified pressure profile. In TENSOR, interior boundaries may slip (this must be specified by the user), but they cannot separate. Exterior boundaries may

be free, rigid, determined by a pressure profile, or "alternating" (the boundary alternates both in space and time from a free to a rigid surface, which acts to disperse a reflected wave).

In both SOC and TENSOR, the interior of a region is assumed for all time to be isotropic and homogeneous. A limitation of the codes results from the fact that the geologic materials are observably not isotropic and homogeneous on a laboratory scale (centimeters) or on a very large scale (kilometers). Only on the scale of problem zoning (meters) are they often homogeneous. Thus, the assumptions of isotropy and homogeneity within a region are probably sufficiently good to obtain the desired accuracy, but we nevertheless lack a good way of going from laboratory measurements on small specimens to zone-valid quantities. If all this is confusing, an example may help to clarify things: Fracture in a laboratory sample is obviously not an isotropic, homogeneous phenomenon, since the sample may completely crack on one or more planes. The same is true of large scale faulting. However, when a meter-sized block of material from a medium that has been explosively fractured is examined, the cracks often have a relatively random orientation.[6] How does one account for this with a credible model? At the moment, the question is sidestepped (as we shall see) by calling a zone "cracked" and not defining a direction. Ultimately, some type of randomized statistical model may be the only way to achieve accurate modeling.

The basic physical process being modeled is: Stress acting for time Δt on a zone gives strain via the appropriate integrals of an equation of motion. Then, some constitutive relation relates the strain to a new stress. This process is carried out for all the zones of a problem, and then time is stepped an additional Δt and the process is begun all over again. This process is continued for as long as is desired, and the result becomes printouts or plots of motion, pressure, shear stress, etc., as functions of position and time. For the sake of brevity, the questions of numerical methodology, i.e., stability, convergence, accuracy, advantages of one differencing method over another, etc., will not be considered here. The numerical treatment of equations of motion and the associated integrations to obtain velocity and displacement are relatively straightforward. General descriptions are given by Richtmyer and Morton[7] and some specific discussion may be found in the articles mentioned in the introduction.

Let us describe a typical SOC or TENSOR calculation in more detail. At the start, energy in some form is fed into the problem. The available options are the expansion of a gas with a prescribed initial energy, pressure or velocity as a function of time at a boundary, and an entire region with an initial velocity or compression. A typical procedure when one desires to simplify a TENSOR problem is to run a one dimensional SOC problem in as close a configuration as possible to the desired two dimensional TENSOR configuration, but for a short time only. In this way the initial and/or boundary conditions for the TENSOR calculation are determined.

Perhaps the most difficult part of the calculational procedure is to relate strain

to a new stress field so that the procedure may be started over again for a new time step. For our purposes, the general relationship of stress, strain, and perhaps internal energy is most aptly called a constitutive relation, although the term equation of state often appears as a hold-over from fluid thermodynamics. An equation of state usually refers to a closed form expression relating pressure, density, and possibly internal energy (or temperature). We shall mean by the term constitutive relation any relation between stress, strain, and internal energy. For a geologic material, the constitutive relation can seldom be written down in closed form.

There are many possible constitutive relations for rocks. Possibly, the simplest is linear elasticity, where the constitutive relation is Hooke's law, which states simply that stress and strain are linearly related by the so-called elastic constants. Even linear elasticity becomes complicated for a non-isotropic material, but for an isotropic material, as we assume, the number of independent constants required by the constitutive relation is only two. A slightly more complex material is non-elastic, but remains elastic for the small changes in stress and strain which occur in a small time step. Such a material might be termed incrementally elastic. In this case, the two required elastic constants must be specified as functions of stress and strain. A much higher order of complexity is the real system in which failure, relaxation, friction, phase changes, and rate and path dependences all drastically complicate the constitutive relations. In general, one must examine the strain state, take into account past history if necessary, and determine if any of the non-elastic processes should occur. This is based on existing theory, laboratory and field measurements, and past successful calculations (if any). Then the new stress state is determined by some combination of table look-up and one or more equations which describe the processes which occur. The determination of a constitutive relation and its application to the codes is the most difficult problem we will discuss.

For the purpose of detailed description, we choose the one dimensional SOC code and spherical symmetry. TENSOR, although more general, will be considered only briefly in a subsequent section. The reason for this choice of action is that the one dimensional framework of SOC is simpler and at first more comprehensible.

SOC Physics in Detail

It is best to picture each SOC zone as a spherical shell with small thickness, as shown in Fig. 3. As a shock wave arrives, propagating from the inside outward, the onset of compression is so rapid that the shell, at first, only compresses, its inertia keeping it from moving outward. Then, as the shock passes through and the shell begins to move outward, it expands. In the following sections, we will assume that the initial conditions have been properly applied. The

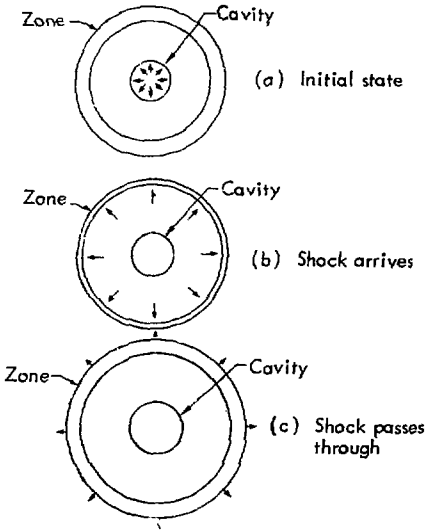

Fig. 3. Progress of shock wave through a SOC zone. The initial state is shown in (a). In (b), the shock wave (shown by arrows) arrives and compresses but does not move the zone. In (c), the shock wave has passed through and the zone is both expanding and moving outward.

stress-strain-constitutive relation loop will be described in detail, and we will see how a problem is initiated. Finally, several sample problems will be presented.

EQUATION OF MOTION

Consider a continuum described by spherical coordinates r, θ, and ϕ. Assume one-dimensional symmetry, where quantities vary only with radius r. The appropriate equation of motion for such a system is

$$\rho \ddot{u}_r = \frac{\partial \sigma_{rr}}{\partial r} + \frac{2}{r}(\sigma_{rr} - \sigma_{\theta\theta}) + X_r, \quad (1)$$

where ρ is density and $\ddot{u}_r$ is acceleration in the r-direction. (A dot indicates time differentiation along a particle path.) Normal stresses in the r and θ directions are given by σ_{rr} and $\sigma_{\theta\theta} = \sigma_{\phi\phi}$, and X_r is a body force. Compressive stresses are defined to be negative in sign. The spherically symmetric system is convenient in that the coordinates r, θ, and ϕ coincide with the directions of principal stress, so that the normal stresses $\sigma_{\theta\theta}$, σ_{rr}, and $\sigma_{\phi\phi}$ are also the principal stresses. Thus, shear stresses such as $\sigma_{\theta\phi}$, $\sigma_{r\phi}$, etc., vanish and Eq. (1) is the only equation of motion. The fact that stresses are purely normal in the principal coordinate system does not mean that there are no shear stresses present. In general, if one considers a plane in the system which does not coincide with a principal axis, then there is shear stress on that plane. In fact, there exists a plane or set of planes for which the shear stress is maximum. The magnitude of this maximum shear stress (in spherical symmetry) is $1/2\,|\sigma_{rr} - \sigma_{\theta\theta}|$. For convenience, define a stress, K, such that

$$K = -\frac{1}{2}(\sigma_{rr} - \sigma_{\theta\theta}), \quad (2)$$

where K is always equal to plus or minus the maximum shear stress. The use of K is convenient because many theories of failure are based on the notion of a limiting maximum shear stress. The text by Jaeger and Cook[8] has a more complete discussion of many of these points.

We wish to rewrite Eq. (1) in terms of K and pressure P, where P is the negative mean stress given by

$$P = -\frac{1}{3}(\sigma_{rr} + \sigma_{\theta\theta} + \sigma_{\phi\phi})$$

$$= -\frac{1}{3}(\sigma_{rr} + 2\sigma_{\theta\theta}). \qquad (3)$$

The combination of Eqs. (2) and (3) yields

$$\sigma_{rr} = -P - \frac{4}{3}K, \qquad (4)$$

and

$$\sigma_{\theta\theta} = -P + \frac{2}{3}K = \sigma_{\phi\phi}. \qquad (5)$$

Equations (4) and (5) show that the principal stresses can be thought of as sums of the negative pressure and a deviatoric stress which is either $-\frac{4}{3}K$ or $+\frac{2}{3}K$. The incorporation of Eqs. (4), (5), and (1) yields, as desired, the equation of motion in terms of P and K:

$$\frac{1}{V}\dot{u}_r = -\frac{\partial}{\partial r}\left(P + \frac{4}{3}K\right) - \frac{4K}{r} - g_r, \qquad (6)$$

where the body force has been written as $-g_r$, the component of gravity in the r-direction, and ρ has been replaced by $1/V$, where V is the specific volume. Equation (6) is convenient for those who like to think in terms of the perhaps more intuitive quantities pressure and shear stress. In the code, Eq. (6) is differenced in the Lagrangian coordinate system, and the appropriate artificial viscosities are added. For our purposes, the use of Eq. (6) as it stands will be more convenient. Equation (6) contains four dependent variables, V, u_r, P, and K, which must be described in terms of the independent variables r and t. As such, we have an underdetermined system of one equation with four unknowns. The physical system must be further described in order to obtain a solution.

VELOCITY-DISPLACEMENT-VOLUMETRIC STRAIN

If we assume that the initial stress state of the system is known, then Eq. (6) can be integrated with respect to time to obtain velocity and displacement, provided that one has an equation describing the relationship between velocity and specific volume. That equation is the equation of continuity, which for our system takes the form

$$\frac{\dot{V}}{V} = \frac{1}{r^2}\frac{\partial}{\partial r}\left(r^2 u_r\right), \qquad (7)$$

where, as before, the dot is the time derivative following a particle path. (Note that only specific volume and not density appears in Eq. (7), since the particle mass remains constant in the Lagrangian system.) Though we now have only two equations in four unknowns, Eqs. (6) and (7) can be solved for V and u_r by assuming a known stress state (values of P and K) at the beginning of each time step. For later convenience, we will define the changed volume of a zone by a quantity mu, the total volumetric strain, where

$$\text{mu} = \frac{V_o - V}{V}, \qquad (8)$$

and V_o is the initial specific volume. The quantity mu increases from an initial value of zero as a zone is compressed. (In several other references, the compression, $\eta = V_o/V$, appears also.)

CONSTITUTIVE RELATIONS

In the previous section, the assumption of a known stress state has allowed a solution for the dependent variables of

the system. If this has been done, we must determine the new stress state. The specification of stress in terms of the other unknowns will require two additional equations. These equations, which complete the system of four equations, are the constitutive relations. For us, the constitutive relations should take the general form

$$f_i(P, K) = g_i(u_r, V) \quad i = 1,2, \qquad (9)$$

where f_i and g_i are any appropriate functions. For a discussion of the requirements, both physical and mathematical, that must be met by a constitutive relation, see Aris.[9] We have mentioned previously that the constitutive relations may incorporate another variable, namely internal energy E, so that Eq. (9) becomes instead

$$f_i(P, K) = g_i(u_r, V, E) \quad i = 1, 2 \ . \ (10)$$

However, for an adiabatic system, the internal energy is strictly a function of the mechanical compression and distortion of the system. This means that we can always write $E = E(u_r, V)$. If this relationship for energy is substituted in Eq. (10), we have again the same form as Eq. (9). Therefore, a constitutive relation of the form Eq. (9) is all that is needed to solve the system, although occasionally we may use Eq. (10) for convenience.

In order to know what type of constitutive relation to apply, the first thing to determine is the state of the material. In SOC, we ask, is the zone under consideration solid, liquid, gas, in a state of "water release," or a high explosive? The initial state is designated by the user; however, changes of state may occur during the calculation, e.g., melting or vaporization, and these changes of state are explained later. Other effects, such as solid-solid phase changes or chemical changes, are not considered. In general, it is not possible to determine constitutive relations entirely by theory. There is, therefore, heavy reliance on experimental data.

Constitutive Relations for a Solid

SOC defines several "sub states" of a solid during loading, unloading, reloading, etc. These sub states are entitled elastic, crushed (special unloading) brittle and ductile failure, and special loading. We will define loading as any increase in the compression of the medium. During loading, pressure is increasing, but not all of the principal stresses are necessarily becoming more compressive. It would perhaps be useful in SOC for the current state of stress to always uniquely determine the current state of strain. In fact, more of the code could be written this way than now is. However, there remains the problem that certain phenomena, such as failure, irreversibly change even the static properties of the material, i.e., a cracked material is generally weaker in shear than an uncracked material, and can sustain no tension at all perpendicular to the crack plane. Therefore, a complicated description of solid behavior is necessary, although we hope to avoid as many nonphysical and therefore inherently nonmeasurable parameters as is possible. Unfortunately, SOC contains several nonphysical parameters.

Initial Stress Calculation—SOC always begins by treating solid zones as incrementally elastic. The two constants used are bulk modulus, k, and either shear modulus, μ, or Poisson's ratio, ν. The bulk modulus is given as a function of pressure by the user, but the other parameter (whichever is used) is assumed constant. To be entirely complete and consistent, SOC should also allow the specification of the shear modulus as a function of P and/or K. This is not done, presumably for the reasons of a prior lack of necessity and the desire for simplicity. For many materials, the SOC assumption of a constant μ or ν works fairly well, but there are certainly classes of material for which shear modulus decreases as a function of pressure, and these cannot be accounted for in the present scheme. (See Eq. (16) below.)

The problem now is to calculate the new pressure $P = P_o + \Delta P$ and shear stress $K = K_o + \Delta K$ after time Δt. This is equivalent to the problem of determining $\dot{P}$ and $\dot{K}$ where the dots indicate time derivatives, since $\Delta P = \dot{P}\Delta t$ and $\Delta K = \dot{K}\Delta t$.

Hooke's law for spherical symmetry takes the well-known form

$$\sigma_{rr} = \lambda\Delta + 2\mu\epsilon_{rr},$$
$$\sigma_{\theta\theta} = \lambda\Delta + 2\mu\epsilon_{\theta\theta} = \sigma_{\phi\phi}, \qquad (11)$$

where λ and μ are Lame's parameters, Δ is the dilatation, which we define as the change in volume divided by the initial volume, and ϵ_{rr} and $\epsilon_{\theta\theta}$ $(= \epsilon_{\phi\phi})$ are the normal strains in the r and θ directions. It can be shown that for infinitesimal strains, Δ is equal to the sum of the strains, such that

$$\Delta = \frac{V - V_o}{V_o} = \epsilon_{rr} + 2\epsilon_{\theta\theta}. \qquad (12)$$

Note that for infinitesimal volume changes with respect to the initial state, $\Delta = -mu$. (See Eq. (8).) Now, if we combine Eqs. (4), (5), (11), and (12), take time derivatives, and rearrange terms, we obtain

$$\dot{P} = -\left(\lambda + \frac{2}{3}\mu\right)\dot{\Delta} = -k\dot{\Delta},$$
$$\dot{K} = -\mu(\dot{\epsilon}_{rr} - \dot{\epsilon}_{\theta\theta}), \qquad (13)$$

where $k = \lambda + \frac{2}{3}\mu$. The definition of strain and the equation of continuity, Eq. (7), give the relationships

$$\dot{\Delta} = \frac{\dot{V}}{V},$$
$$\dot{\epsilon}_{rr} = \frac{\partial u_r}{\partial r}\dot{\epsilon}_{\theta\theta} = \frac{u_r}{r}, \qquad (14)$$

and using Eq. (14) in Eq. (13) gives the final form of the elastic constitutive relations

$$\dot{P} = -k\frac{\dot{V}}{V},$$
$$\dot{K} = \mu\left(\frac{u_r}{r} - \frac{\partial u_r}{\partial r}\right). \qquad (15)$$

Equation (15) contain two constants, k and μ, and apply for small changes only, but since we assume incremental elasticity, Eq. (15) apply for any succession of small changes, provided that the appropriate values of the constants as functions of P and K are given. In SOC, we assume, as mentioned above, that k takes on a value as given by the user and that μ is either a constant given by the

user or calculated from a constant Poisson's ratio (also given by the user) and the basic relationship

$$\mu = \frac{3}{2} k \left(\frac{1 - 2\nu}{1 + \nu} \right) . \qquad (16)$$

Note that Eq. (16) causes μ to increase as k increases. In SOC, the value of μ that is specified by the user or calculated from Eq. (16) is multiplied by a weighting factor, wt, given by

$$wt = \frac{E_F - E}{E_F} , \qquad (17)$$

where E_F is the internal energy per unit volume required to melt the material (a user-input quantity). The use of wt is simply an attempt to grade the shear resistance of the material to zero at melting. Values of k are effectively specified by providing an experimentally determined table of P versus mu or P versus V. This means that the first equation of (15) may be replaced by

$$P = P(mu) . \qquad (18)$$

This is the P-mu loading curve, which should be the hydrostat for the material.

There are two popular techniques for obtaining loading data. One is to reproduce shock conditions with an explosive or by the impact of a projectile. The other is to squeeze the material quasi-statically in a hydraulic press, assuming that the much greater strain rate of shock loading can be ignored. To obtain P-mu curves for SOC, both of these techniques are used, the quasi-static up to about 50 kbar, and shock loading beyond.

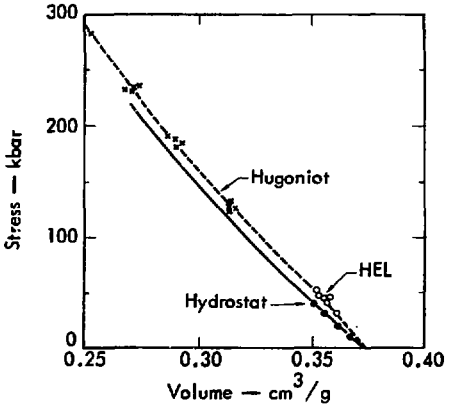

Fig. 4. Comparison of Hugoniot and hydrostat for hardhat granite.[2] HEL is the Hugoniot elastic limit.

Shock loading causes a sudden increase of stress on all axes. However, the strain is discontinuous essentially along the axis of shock propagation only. A state of strain-increase on one axis only is called uniaxial strain. The locus of points representing the possible states of shock loading in the stress-volume plane is often called the Hugoniot. In quasi-static experiments, one usually measures the hydrostat, which is simply the loading curve in the pressure-volume plane for hydrostatic conditions (no deviatoric stress). Only if the material behaves always as a fluid would the Hugoniot and the hydrostat be superimposed. In general, the hydrostat lies below the Hugoniot, as shown in Fig. 4. However, the Hugoniot can be converted into the equivalent hydrostat as follows: If the loading Hugoniot is assumed to represent a state of uniaxial strain

($\epsilon_{\theta\theta} = \epsilon_{\phi\phi} = 0$), then the following relations hold for the Hugoniot if linear elasticity is assumed:

$$\sigma_{rr} = (\lambda + 2\mu)\epsilon_{rr} ,$$

$$\epsilon_{rr} = \Delta . \qquad (19)$$

For the hydrostat,

$$P = \left(\lambda + \frac{2}{3}\mu\right) \Delta . \qquad (20)$$

So, the difference between the Hugoniot ($-\sigma_{rr}$) and the hydrostat (P) for the same Δ is

$$\text{Hugoniot - Hydrostat} = -\frac{4}{3}\mu\,\Delta = -\frac{4}{3}\mu\left(\frac{V - V_o}{V_o}\right) . \qquad (21)$$

The behavior implied by Eq. (21) is expected up to the Hugoniot elastic limit (HEL). Figure 4 gives an example for a granite. Above the HEL the material fails, along with our assumption of linear elasticity, and the shear stress no longer increases. However, $-\sigma_{rr}$ and P now increase at the same rate, so the difference between the Hugoniot and the hydrostat remains constant above the elastic limit. One should therefore maintain, above the HEL, the difference between the Hugoniot and the hydrostat that is experimentally observed at the HEL (Fig. 4).

What of unloading? The code assumes that high pressure unloading occurs along the loading path. However, if observed in the laboratory with quasi-static equipment, unloading is isothermal, while shock unloading is more nearly adiabatic. Through the range of laboratory measurement (50 kbar) this is but a small problem, because there is not much heating in a 50-kbar shock. The realm of importance for the adiabatic-isothermal discrepancy is in the pressure range from 100 kbar, up to vaporization at about 1000 kbar. Currently, it is assumed that the errors in the experimental work are such that the differences between the loading Hugoniot, the unloading adiabat, and laboratory isotherms are insignificant. This, of course, will not remain a good assumption with increases in the accuracy of experimental data and a desire for improved calculations.

Crushing and "Special Unloading" — The initial or trial values of P and K have now been calculated from the appropriate elastic relationships. What reasonable modifications to the elastic state must we consider? The first is called crushing.

Suppose that the material has been loaded to a total volumetric strain called mu_{max}, and unloading has just begun (e.g., the peak of the pressure pulse of a wave has just gone past). The code now checks for the occurrence of crushing. The crushing model in SOC is loosely based on the concept of a material that is composed of a solid matrix with included void space (pores). Upon loading, the pores collapse until they are closed (or at least partly closed). Therefore, upon unloading, if the crushing is to some extent irreversible, the material cannot return to its original volume. The effect of crushing is assumed to be a function of P only, which is reasonably consistent with data, although not completely general. If the user desires this type of behavior (typified by a material

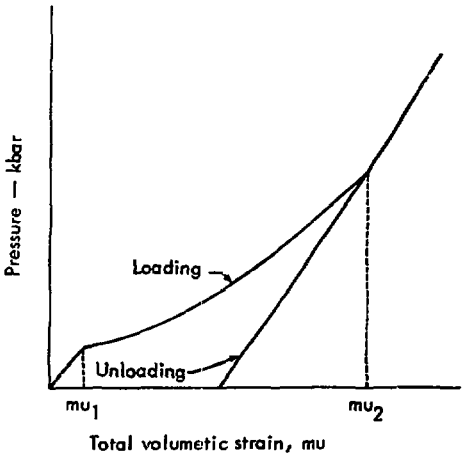

Fig. 5. Typical loading and unloading curves in P-mu space.

like alluvium) he must provide a P-mu unloading curve, which differs from the initial loading curve.

Typical loading and urloading curves are shown in Fig. 5. In addition to these curves, two points are specified by the user. They are mu_1, the value of mu up to which the material is to be treated elastically, i.e., the initial increment of compression elastically deforms the matrix without permanently collapsing pores, and mu_2, the point at which the loading and unloading curves merge, and beyond which no further crushing occurs. Between the points mu_1 and mu_2, crushing behavior occurs.

Suppose that all the necessary curves and points have been supplied and unloading from mu_{max} is beginning. First, mu_{max} and mu_2 are compared. If $mu_{max} \geq mu_2$ (crushing is complete), then the unloading curve is followed, and only the unloading curve is used in subsequent calculations. On the other hand, if $mu_{max} < mu_2$ then only partial crushing has occurred, but we first check if $mu_{max} < mu_1$. If this is true, then crushing has not yet been initiated, and the material is treated elastically. Now, if $mu_1 < mu_{max} < mu_2$ a routine is entered which is called "special unloading" (even though it includes subsequent reloading).

Special unloading accounts mathematically for partial crushing by modifying, at each time step, the slope of the P-mu curve. There are several physical models of porous materials that might be employed here. SOC, unfortunately, uses a scheme based primarily on geometrical reasoning. First, one defines a slope slp_1

$$slp_1 = slp_{load} + \frac{mu_{max}}{mu_2} \times (slp_{unload} - slp_{load}) , \qquad (22)$$

where slp_{load} and slp_{unload} are evaluated at the current pressure. The value of slp_1 is in general between the values of slp_{load} and slp_{unload}. For $mu_{max} \to mu_2$, $slp_1 \to slp_{unload}$, and for $mu_{max} \to mu_1$, where $mu_1 \ll mu_2$, $slp_1 \to slp_{load}$. Then, to determine the new slope slp, slp_1 is modified as follows

$$slp = slp_1 - \frac{mu_1}{mu}(slp_1 - slp_o) , \qquad (23)$$

where slp_o is the first slope of the loading curve. The main effect of the Eq. (23) modification of Eq. (22) is that $slp \to slp_o$ if $mu \to mu_1$ upon unloading. If unloading proceeds to $P < 0$, all slopes are straight-line extrapolated from their $P = 0$ values. Reloading follows Eq. (23)

until mu = mu_{max} is reached and then continues up the loading path until another unloading occurs, and then the process is repeated, but for the new value of mu_{max}.

The behavior described by SOC's special unloading scheme only crudely approximates some of the existing laboratory data. That this model is not better founded is unfortunate, because the specific nature of the P-mu loading-unloading model causes much of the energy-storing hysteresis in the medium. This hysteresis, in turn, may critically determine the attenuation of a shock wavefront. It is a deficiency of both SOC and TENSOR that several of their models of material behavior lack true physical meaning.

Failure—In the laboratory, and in situ, one observes a very obvious nonelasticity in rocks, i.e., at some point they fail to maintain the ability to support the stresses placed upon them. The description of the exact conditions under which such failure occurs has remained a problem, particularly for mining and construction engineers, for years. We will first discuss the general characterization of failure in rocks, and then separate the discussion into sections on brittle failure and ductile failure, although the physical mechanisms of the two types of failure may be similar in rocks.

For many rocks, it has been observed[10] that the point of ultimate failure in K-P space does not depend upon the loading path in that space and is dependent only on K, the maximum shear stress. Then, if rate effects are neglected (dependence on $\dot{K}$ or $\dot{P}$) we may hopefully define a failure surface in K-P space. If the loading path touches this surface, failure is defined to occur, and the shear stress is either limited or relaxed according to a scheme to be discussed in the following sections.

Let us take a closer look at K-P space in order to define the failure surface. (We persist in calling it a surface even though two variables clearly define only a line. However, a three dimensional generalization of the same notions leads to a true surface.) Most laboratory tests are performed on a cylindrical sample as shown in Fig. 6. An axial load is applied with a piston and the sample is enclosed in a fluid medium which applies a confining pressure. This is called a triaxial test. Since the directions of principal stresses, σ_z, σ_x, σ_y, coincide with the axes of the sample and $\sigma_x = \sigma_y$, we may think of these principal stresses in the same way that we do the three SOC

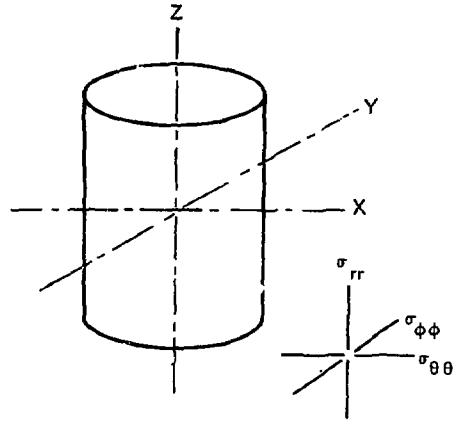

Fig. 6. Geometry of cylindrical sample for laboratory tests compared with the equivalent SOC spherical coordinates.

principal stresses σ_{rr}, $\sigma_{\theta\theta}$, $\sigma_{\phi\phi}$, where $\sigma_{\theta\theta} = \sigma_{\phi\phi}$. Note that the stresses in these two systems are not necessarily identical, but that the systems may be considered equivalent in the sense that they both contain two equal principal stresses.

In most laboratory apparatus, we cannot easily apply tension to a sample. Therefore, all of the principal stresses are negative and P is positive. This limits us to two basic types of tests. We may have a greater axial load than confining pressure where K is positive, which is called compression, or, we may have a greater confining pressure than axial load where K is negative, which is called extension. The terms compression and extension refer to the effect of such loading on the dimensions of the cylinder. Equations (2) and (3) relate P, K, and principal stresses. In K-P space, compression occurs above the P axis and extension below it (Fig. 7). The line K = 0 is hydrostatic compression. Uniaxial compression ($\sigma_x = \sigma_y = 0$) and uniaxial extension ($\sigma_z = 0$) are the limits in K-P space which can be investigated with the apparatus as described. Furthermore, since we usually apply a considerably greater load with the piston than we can with the confining fluid, the investigatable area extends much further to the right above the P-axis than it does below. Given these limitations on much of the experimental data, what may we observe from experimental data about failure in the brittle rocks?

If typical failure surfaces are reflected across the P axis (Fig. 8), they generally resemble one another but do not coincide. The magnitudes of K at the

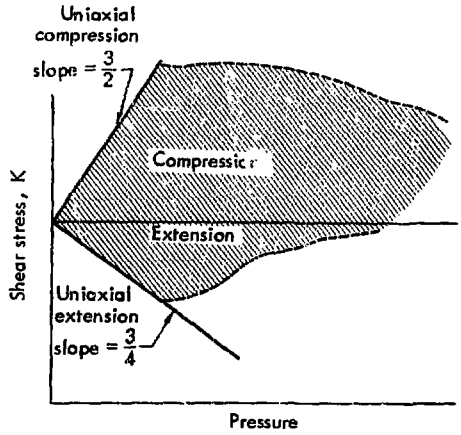

Fig. 7. Schematic representation of K-P space. Shaded area is the approximate limit of commonly investigatable area.

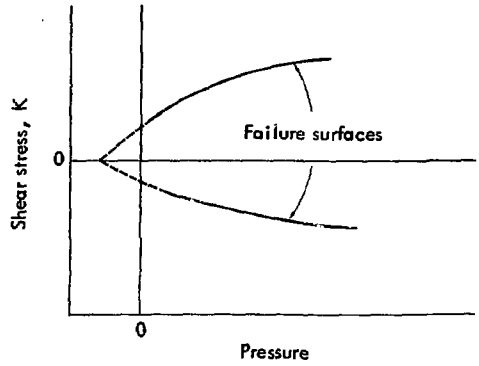

Fig. 8 Typical failure surfaces in K-P space. Material in a stress state between the surfaces does not fail.

surfaces are also observed to increase monotonically as P is increased. This means that rocks can sustain more shear as pressure is increased, which makes sense if one envisages a mechanism of

failure that involves crack separation and sliding friction between interfaces. The increasing pressure then makes it more difficult for separation and/or sliding to occur. We have one more bit of good experimental information—namely that in those few tension tests which have been made ($\sigma_x = \sigma_y = 0$, σ_z positive), rock has been observed to be very weak. If one extrapolates the existing curves into the tension region, the general picture of a failure surface in K-P space emerges as shown in Fig. 8. For SOC, we wish as a simplification to supply only one failure curve, rather than separate curves for compression and extension. This is particularly desirable because there is much more compression than extension data (particularly at high pressures). A method of doing this will be discussed in the following paragraphs.

If one pictures the three principal stresses (σ_1, σ_2, σ_3) as having, in general, three different values, then one would expect that the failure surface would depend on all three stresses (which is why we call it a surface). In the tests we have mentioned (triaxial compression and extension), two of the principal stresses are equal. In the first case the two equal stresses are the greatest, and in the second they are the least. This means that the intermediate principal stress has either its largest or smallest possible value in one or the other of these tests. Let us first assume that there is no effect from this change in intermediate principal stress. This means that failure depends only on the maximum shear stress $|K|$ seen by the material and is independent of the variation of shear stress with angle. In effect, it is the description of a three-dimensional process with a two-dimensional model. Even then, the failure surfaces for extension and compression do not coincide on a $|K|$-P plot, so to say that the surfaces are the same is <u>not</u>, as one might first assume, the simplest correct assumption.

Let us examine this more carefully. We will assume that the mechanisms and the corresponding stress values are the same for compression and extension failure. At failure,

$$P_c = -\frac{1}{3}(2\sigma_1 + \sigma_3),$$

$$|K| = \frac{1}{2}(\sigma_1 - \sigma_3), \quad (24)$$

$$P_e = -\frac{1}{3}(\sigma_1 + 2\sigma_3),$$

where c indicates compression and e extension. Therefore, for any particular value of $|K|$, the difference in position on the P axis is given by

$$P_c - P_e = -\frac{1}{3}(\sigma_1 - \sigma_3) = -\frac{2}{3}|K| . \quad (25)$$

So, on a $|K|$-P plot, as shown in Fig. 9, typical values (in this case for Solenhofen Limestone) for failure in extension should lie to the <u>right</u> of the values for compression, and they do. This observation is consistent with laboratory data on many rocks.

Is there a possible variable other than P that would allow a single surface for compression and extension in the case of the above assumptions concerning the stresses? This would be a worthwhile simplification of the type we are looking for. We ask if there is a linear combination of P and K, call it $\bar{P}$, such

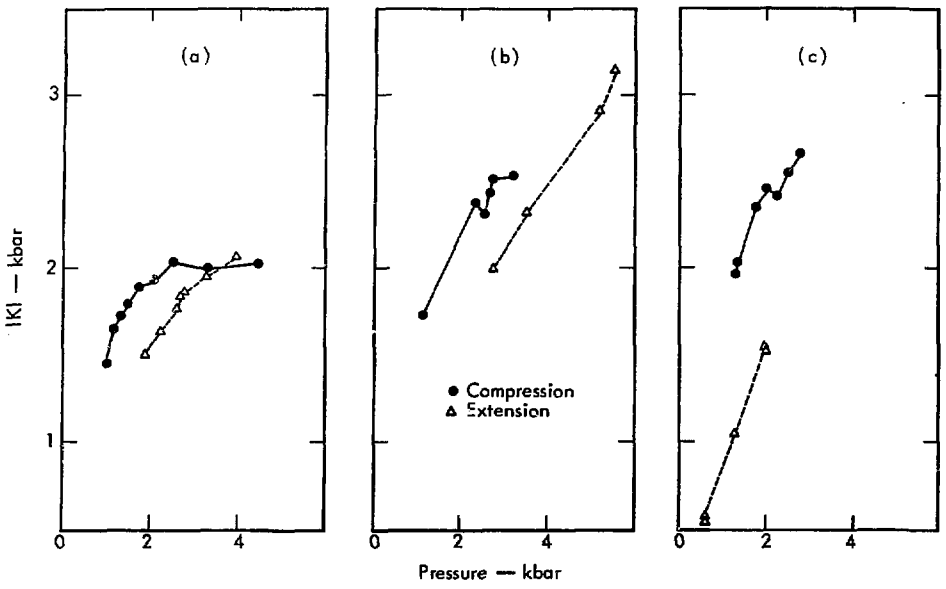

Fig. 9. Experimental results for failure in Solenhofen limestone, shown in $|K|$-P space. Data in (a) are from Mogi,[11] and in (b) and (c) are, respectively, from Blocks 3 and 5 of Handin, Heard, and Magouirk.[12]

that $|K|$ plotted against $\bar{P}$ produces superposed surfaces for compression and extension failure. This is the same as solving the following equation for the constant, a,

$$P_c + aK_c = P_e + aK_e , \qquad (26)$$

where, in compression, $K_c = \frac{1}{2}(\sigma_1 - \sigma_3)$, and in extension, $K_e = -\frac{1}{2}(\sigma_1 - \sigma_3)$. The solution of Eq. (26) is a = 1/3. Therefore, we would expect that a plot of $|K|$ versus $\bar{P}$ where $\bar{P} = P + K/3$ should produce identical failure surfaces in compression and extension if intermediate principal stress has no effect on failure. Figure 10 shows such $|K|$ versus P plots for the same samples as Fig. 9. The results do tend more toward one curve when $\bar{P}$ is used, and the $|K|$-$\bar{P}$ representation appears usefully accurate to within the variability of results from one sample to another. Cherry and Petersen[2] reach the conclusion to plot $|K|$ versus $\bar{P}$ via a somewhat different line of reasoning. They show that the data of Mogi[11] when plotted as $|K|$ versus $\bar{P}$ produces "acceptable" superposed curves (Fig. 10). SOC therefore uses as input a table of values of $|K|$ and $\bar{P}$. Most of the laboratory data for the tables is obtained from triaxial compression tests. Data for tension and very high compression are either extrapolated or guessed.

There are at least two objections to the above procedure. The first is that

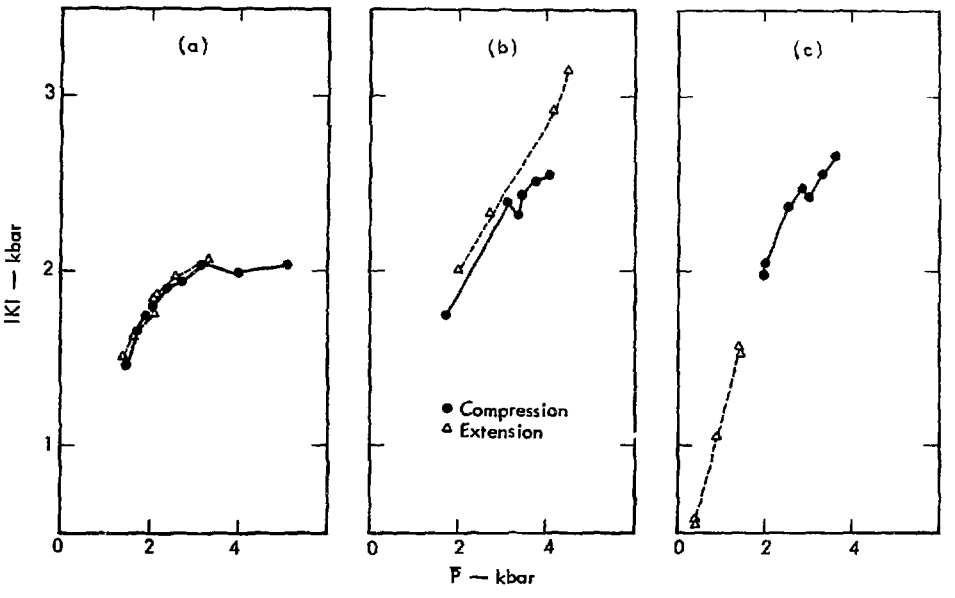

Fig. 10. Experimental results for failure in Solenhofen limestone, shown in $|K|$-$\bar{P}$ space. Data are the same as in Fig. 9.

failure obviously should depend to some extent on the intermediate principal stress. Mogi[11] shows that this is true experimentally, though the effect is usually small. One would certainly expect this result from a sufficiently general theory. Most theories, however, have stemmed from two dimensional considerations, e.g., Griffith's failure criteria. (See Jaeger and Cook.[8]) These theories, by their very nature, contain only two principal stresses. The relative ease of the general application of such theories to three dimensional media and the three dimensional media and the tremendous additional complication of involving all three stresses generally make it desirable to be able to ignore the intermediate stress until data compels us to include it.

The second objection to the use of $\bar{P}$ has been mentioned by White.[13] He states that to force the superposition of failure surfaces for compression and extension in $|K|$-$\bar{P}$ space causes, in $|K|$-P space, an unreal "separation" before the ductility-caused "coming together" as shown in Fig. 11. This separation occurs because extension and compression curves must always be separated by $|K|/3$ on the $\bar{P}$ axis. The validity of White's objection can neither be proven nor disproven from the data of Fig. 9. A subsidiary point of White's is that the $|K|$-$\bar{P}$ representation forces compression and extension curves to be equally

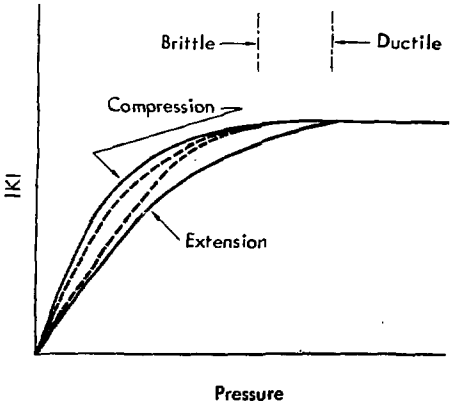

Fig. 11. Hypothetical failure surface in $|K|$-P space. Solid lines are for assumed validity of the $|K|$-P representation. They are separated on the P-axis by $|K|/3$. Dashed lines are White's[13] claim of the actual appearance of data.

spaced about the torsion failure curve. (Torsion, for our purposes, may be defined as $\sigma_2 = \frac{1}{2}(\sigma_1 + \sigma_3)$.) He says that this is not experimentally observed. However, the possible SOC stress states are only compression and extension, thus the torsion objection is not of crucial importance to SOC. It seems that the major overall objection to the use of $\bar{P}$ is a lack of complete generality. In the past, this did not matter, but as laboratory and field data become more abundant and the detail required of calculational results increases, we will probably need a more general description.

A good general system for representing the state of stress of a material and the complete failure surface has been proposed by White.[14] His scheme describes the stress state in terms of I_1, the first stress invariant, and I_{2d} and I_{3d}, the second and third deviatoric invariants. In all cases, I_1 is the equivalent of pressure, and in the case of SOC, $I_{2d} = 4/3\ K^2$ and $I_{3d} = 16/27\ K^3$. So we see that for SOC, we can look at I_1 as giving P, I_{2d} as giving the magnitude of K, and I_{3d} as giving the sign of K (although both magnitude and sign could be obtained from I_{3d}). The usefulness of this system is that when plotted in I_1, $I_{2d}^{1/2}$, $I_{3d}^{1/3}$ space (Fig. 12), the boundaries for compression, extension, and torsion are straight lines, and the failure surface can probably be represented by a low degree polynomial. We must remember that, where only compression or extension are allowed, as in SOC, there is little practical difference between White's or the existing system. The major advantage of the invariant system lies in its possible multidimensional applications, such as the TENSOR code.

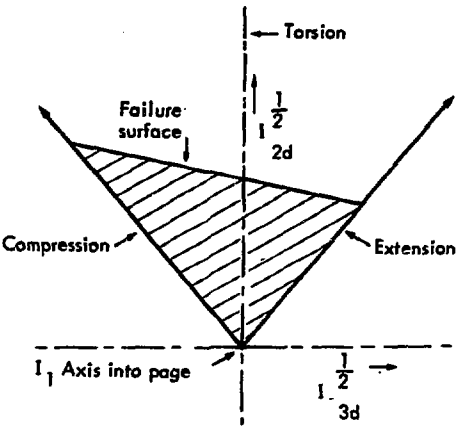

Fig. 12. Invariant geometry for description of the failure surface. The shaded area represents allowable stress states.

Brittle Failure or "Cracking"—Assume that a failure surface has been provided by the user in the form of a table called the K-f^s loading curve. We now wish to describe the behavior of material that has been loaded to the failure surface for the first time. (In some cases, the failure surface may never be reached. Then, of course, special procedures for failure are never required.) In the laboratory, one observes the violent growth of a crack, or many cracks, and the sample suddenly loses its ability to sustain shear or tensile stress. A "stress relaxation" occurs. In the field, one observes anything from microfracture to a general breaking up of the rock material and severe attenuation of waves which pass through it. One infers that the stress relaxation observed in the laboratory accounts for the attenuation observed in the field. From an energy point of view, we can any that some of the kinetic energy that has been converted into strain energy and/or heat is never returned to the motion of the medium.

How shall stresses be relaxed when brittle failure occurs? We assume that for material which has not failed previously and is not in tension, that only the shear (or deviatoric) stress relaxes. Two quantities must then be established, namely, the rate of relaxation and the "equilibrium value" toward which K is relaxed. Perhaps the simplest relaxation model that has a physical interpretation is that of a Maxwell solid. If an elastic solid can be represented by a spring, then the Maxwell solid is given by a spring in series with a dashpot. In SOC notation, the equation for $\dot{K}$ in Eq. (15) should be replaced by the equivalent equation for a Maxwell solid

$$\dot{K} = \mu \left(\frac{U_r}{r} - \frac{\partial U_r}{\partial r} \right) - \frac{\mu}{\eta} (K - K_o), \quad (27)$$

where the relaxation rate is given by η, the viscosity of the material associated with brittle failure, and K_o is the equilibrium value of K. Equation (27) is convenient in that it has a rough physical interpretation, that is, a similar equation is obtained from a dislocation theory of failure.[15] The viscosity can then be associated with the plastic strain rate. Unfortunately, this physical description probably applies best to metals and single crystals, and not to rock, where failure is initiated and determined by, for example, intergranular sliding, degree of cementing, etc. Nevertheless, Eq. (27) is convenient and does in general produce an exponential stress relaxation, which is a sufficient way to reproduce the scanty data on relaxation in rocks. In support of the attitude that Eq. (27) is usually adequate, is our observation that the most critical effect of failure models on code calculations is in their limitation of the shear stresses, and not in the exact rate of stress relaxation (provided that the relaxation rate is not so rapid as to cause numerical instabilities). A definite disadvantage of Eq. (27) is that it is effectively a high-pass filter. Often we would prefer a low-pass filter in order to produce high-frequency attenuation.[16]

The correct way of applying Eq. (27) would be to difference it according to the SOC scheme and then to use the new equation as the appropriate constitutive

relation. SOC, however, uses a cruder approximation, and that is to compute the elastic value of K from Eq. (15), call it K_e, and then relax K_e back each time step according to the relation

$$K = K_e \left(1 - \frac{\mu}{\eta} \Delta t\right), \tag{28}$$

where the relaxation rate μ/η is obtained from a scheme described in the next paragraph, and relaxation is toward $K = 0$. It can be shown[16] that Eq. (28) represents Maxwell relaxation only over a narrow range of wavelengths, or frequencies, and that in general Eq. (28) relaxes K somewhat too quickly as compared to Eq. (27). Of course we could easily argue that we know so little, and have so few measurements, that the exact form of relaxation hardly matters. This leads immediately to the conclusion that Eq. (28) is the more desirable form, since we have already calculated K_e, and need apply only a simple correction. This argument has considerable validity, because we can only guess at the appropriate value of viscosity anyway. However, as our knowledge improves, our mathematical representation must eventually improve also.

SOC attempts to give brittle failure, and in particular the viscosity term in Eq. (28), a more literal interpretation in terms of the "cracking" of the material. When the failure surface (K-$\bar{P}$ loading curve) is reached, a crack is assumed to initiate in the zone with a velocity C given by Bieniawaski.[17] This velocity is somewhat less than the shear velocity in the material. No physical crack actually occurs in the calculational grid, but stress is relaxed according to Eq. (28) with the viscosity term given by

$$\frac{\mu}{\eta} = \frac{CL}{(4\Delta R)^2}, \tag{29}$$

where ΔR is the zone dimension and L is a "crack length" given simply by

$$L = Ct, \tag{30}$$

where t is the time beginning at crack initiation. The quantity L is allowed to enlarge with time until it is equal to $4\Delta R$. At this point, a comparison of the relaxed stress is made with another user provided curve, the K-$\bar{P}$ unloading curve. This curve is meant to represent the failure surface for previously failed material, which is presumably weaker than it was originally. The user could use the same curve as his original failure surface if he did not prefer the weakening. At any rate, the relaxed stress is checked to see if it is less than 1/2 the K-$\bar{P}$ unloading stress. If it is, the crack is deemed complete, and the code returns to the uncracked routines, except that the fact that the material has previously failed has been stored. If the stress has not relaxed to 1/2 of K-$\bar{P}$ unloading, then the failure routine continues until that value is reached, and only then is failure complete. Note that Eq. (28) implies relaxation toward $K = 0$, but that the code stops the process sooner. This procedure is modified if any of the principal stresses is tensile (greater than zero), in which case the crack velocity is multiplied by a factor of 12, under the assumption that tensile failure is more rapid than shear failure.

There are some further complications to the above procedure. If the initial

crack is forming, K could conceivably be incremented upward on some time steps. In this case, there is a limiting upper value of K given by wt · K_{max} where K_{max} (maximum shear stress) is a user-provided quantity and wt is the same fluid weighting factor from Eq. (17) that we have seen previously applied to the shear modulus. As we shall see later, the quantity K_{max} is also the limiting value of K used for ductile failure. Thus, the brittle failure routine must relax the shear stress immediately to at least its value for ductile failure. This modification is not applied to the second or subsequent cracks, because K must already drop at least to the K-$\bar{P}$ unloading curve. Also, both the loading and unloading failure curves are multiplied by wt to reflect the fact that the shear stress should approach zero at the melting point.

In general, subsequent failure is treated in the same way as just described, except that the failure surface is now the K-P unloading curve. There are, however, three exceptions, as we will now describe. Suppose that the material is in some state of initial or subsequent failure. First, consider the case in which the principal stress with the greatest magnitude is tensile. This case corresponds to the condition $\bar{P} < 0$. The code now requires that failure occur very rapidly, and that the zone be prevented from sustaining any stress at all, i.e., the zone "comes apart." Thus, the normal relaxation scheme is bypassed and both I and K are simply set to zero. The second special case is similar, but it occurs when the mean stress is tensile ($P < 0$). In this case, P and K are also set to zero, with the bypass of normal relaxation. The third special case involves another user provided quantity, mu_o, the "bulking factor." If the total volumetric strain mu is less than mu_o, where mo_o is usually negative, then the material "bulks," or becomes disoriented rubble. In this case, we also set K = P = 0 and bypass normal relaxation. If any of the special cases of failure has occurred, the code henceforth uses only a routine called "special loading," which will be described in the next section.

Whether there is any physical reality in the cracking description of stress relaxation as described by Eqs. (28), (29), and (30), and the subsequent paragraphs is questionable. Because no real crack is actually formed, "cracking" is just the name of the stress relaxation scheme. Altogether, this scheme appears to depend on about 10 parameters, some of which are dependent. Several of these parameters such as the K-$\bar{P}$ unloading curve, mu_o, and K_{max}, are difficult to measure or predict, and one of the parameters (the zone size) is completely without physical meaning. A finite-difference approximation, in the limit of vanishing zone size, should approach the partial differential equation it represents. The effect of vanishing zone size on Eqs. (28) and (29), as they operate in the code, is uncertain. What we witness in SOC is apparently a procedure that has grown over a period of several years into something much more complicated and less physical than was originally intended. SOC, however, does appear to produce acceptable results for the materials and conditions for which it was originally developed. Cherry and

Petersen,[2] for example, point out that there is some agreement with relaxation data for granite (for a problem run using "standard" zoning). This might result from the arbitrary choice of four zones for relaxation as well as anything else. We have no confidence in predicting that the SOC failure description will work in a previously unknown material under untested conditions. It is more desirable to have a relaxation model consistent in complication with our understanding of the phenomenon, containing perhaps two or three parameters that can be correlated with the actual behavior of different materials under many conditions. To describe quantities called, for instance, "crack length" and then to render them meaningless by connecting them with the zone size simply confuses the issue and is numerically unsound.

"Special Loading"—The special loading routine is entered if failed material sees either $\bar{P}$ or P less than zero, or $mu < mu_o$. The simplest case of special loading occurs if P, at each time step, tends to remain less than zero. Then, both P and K continue to be zeroed. The more complicated cases occur for reloading with $P > 0$. The purpose of special loading is to modify the calculation of P such as to take into account the apparent increase of material volume due to the separation of cracks and opening of voids. (The K calculation is unchanged.) Upon reloading, the P-mu curve must eventually merge back into the P-mu loading curve, but we would like this to be a gradual process as the material reconsolidates. The scheme which SOC uses is, as with the case of crushing, apparently chosen from geometrical considerations only and not from a more physical model of material behavior.

Assume at first that there is no P-mu unloading (crushed) curve for the material (Fig. 13), and that we are at some positive pressure. Pressure, however, may have been zeroed in the past, so we are not necessarily on the initial P-mu loading curve. There are three possible special loading paths. If mu is greater than it would be if it were at the current pressure on the initial P-mu loading curve ($mu > mu_{load}$), SOC calculates the new slope of the loading path as

$$slp = slp_{load} . \qquad (31)$$

Thus, slp is the same as for the initial loading curve. The loading path defined by Eq. (31) will always remain below and parallel to the initial curve, without merging with it. In this case, SOC does not achieve the desired behavior.

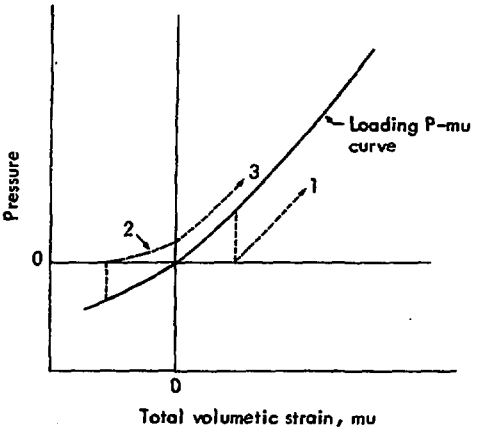

Fig. 13. "Special loading" behavior for the case of no crushing. Path 1 is given by Eq. (31), 2 by Eq. (32), and 3 by Eq. (33).

The second possibility is that $mu < mu_{load}$ and $mu < 0$. SOC then calculates

$$slp = slp_{load}\left(\frac{mu - mu_o}{mu_{load} - mu_o}\right)^2, \quad (32)$$

where mu_o is the bulking mu as defined previously. (If $mu < mu_o$, the pressure will simply be zeroed, so we are concerned here only with the case $mu_o < mu < 0$.) The squared factor in Eq. (32) is usually small but approaches unity as mu approaches mu_{load}. It turns out that Eq. (32) gives the desired merging behavior, because, on the negative mu axis near to mu_o, reloading is at a very small angle with respect to horizontal, but, as $mu \to 0$, slp becomes closer to, but less than, slp_{load}, as desired. Suppose reloading has occurred as described, and mu has become positive, but it still lies above the initial loading curve. Then, we have the third possibility, that $mu > 0$ and $mu < mu_{load}$. The code treats this by setting

$$slp = slp_{load}, \quad (33)$$

which causes loading to be above the elastic curve, thus not achieving the desired behavior.

Now, consider the same problem, but for the case where the user has specified a P-mu unloading (crushed) curve as well. There are now four possibilities (Fig. 14). First, we have the possibility that $mu > mu_{crush}$. If so, SOC uses

$$slp = slp_{crush}, \quad (34)$$

which causes loading below the crushed curve, which is not correct. The second

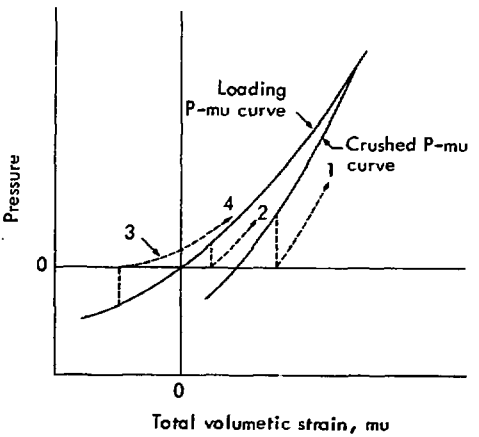

Fig. 14. "Special loading" behavior for the case of crushing. Path 1 is given by Eq. (34), 2 by Eq. (35), 3 by Eq. (36), and 4 by Eq. (35).

possibility is $mu < mu_{crush}$ and $mu > 0$. Then we lie between the initial loading and crushed curves and load between them according to

$$slp = slp_{load} + \left(\frac{mu - mu_o}{mu_{crush} - mu_o}\right)^2 \times (slp_{load} - slp_{crush}), \quad (35)$$

which produces a curve with the correct geometry. The third possibility is $mu < mu_{crush}$ and $mu < 0$. Then we load according to

$$slp = slp_{crush}\left(\frac{mu - mu_o}{mu_{crush} - mu_o}\right)^2, \quad (36)$$

which is the same as Eq. (32) except that slp_{load} is replaced by slp_{crush}. This relationship produces the desired behavior in much the same way as Eq. (32).

For reloading the mu > 0, we now have the fourth possibility, in which mu > 0 and mu < mu_{load}. In this case, SOC uses Eq. (35) which produces a path that tends slowly back toward the initial loading curve, as desired.

If a crushed P-mu curve is specified which lies below the original loading curve, the special loading behavior seems to be at least qualitatively adequate except in the case where mu > mu_{cr}. Then Eq. (34), which defines the subsequent behavior, is clearly not adequate. The case mu > mu_{cr} could occur only if *the pressure is zeroed from a point* beyond which the crushed P-mu curve crosses the P=0 axis. Since this occurs in general for positive pressures, the zeroing can occur only from the $\bar{P} < 0$ criterion. An examination of the statements in the previous section reveals that $\bar{P} < 0$ and $P > 0$ occur simultaneously only for a state of extension and a limited range of parameter values. For the parameters normally specified (in particular, typical values of the failure surfaces and P-mu curves), the occurrence of the above peculiarity is extremely rare, and even so, it might appear only as noise imposed in a normal calculation. Nevertheless, the possibility indicates a lack of generality which should not exist.

Ductile Failure—Ductile failure (yield), is the most common failure mechanism in metals and plastics, but it occurs in most rock materials only at high pressures and temperatures. If failure is ductile, a limiting shear stress is observed, as for brittle failure. If one attempts to increase the shear stress above the limiting value, the material simply deforms without allowing an increase in the shear stress. There is, however, little tendency to relax below the limiting value. We assume that ductile failure affects only K and not P.

SOC uses a very simple and mostly adequate model of ductility. First, in K-$\bar{P}$ space, the user specifies a value of $\bar{P}$, called P_1, at which the brittle-ductile transition occurs. If $\bar{P} > P_1$, the brittle failure routine is ignored, and K is set equal to itself or

$$K = wt \cdot K_{max}, \qquad (37)$$

whichever is smaller. The quantity K_{max} has been mentioned previously in conjunction with brittle stress relaxation. No other adjustments are made. If the material has previously failed in a brittle manner, all brittle "cracks" are assumed to heal. Any subsequent reloading is as for a new uncracked elastic material except that the code remains in special loading if it was in it to begin with. SOC does not account for ductile strain hardening, in which K_{max} increases as yield occurs. For rocks, this is probably *not a crucial shortcoming, because* ductile failure is not common at low pressures. Furthermore, at very high pressures, the existence of hardening is probably not significant with respect to calculational accuracy.

An important problem for SOC is the nature of the transition from brittle to ductile failure. Microscope examination shows that failed rock exhibits both brittle and ductile phenomena, even if, macroscopically, the failure appears entirely brittle or ductile.[18] The transition should therefore not be as sudden as

SOC treats it. The best model to use may well be some combination of brittle and ductile failure, or it may be better to rearrange the entire approach to failure by going to a more microscopic and perhaps randomized model with statistical averaging to obtain bulk properties. Currently, it is possible for two adjoining points in the same SOC continuum to be, respectively, entirely brittle and entirely ductile, and this type of discontinuity is always numerically unsound and often physically unsound. If such discontinuities must arise, e.g., a first order phase transition, they must be handled with the appropriate boundary conditions.

Other Non-Elastic Processes—We have discussed, thus far, primarily the end product of non-elastic effects, i.e., failure. SOC does not consider non-elasticity, other than crushing, which may preceed failure. (An exception is the forced decrease of shear modulus as melting is approached.) Presumably, even brittle failure is to some degree a gradational process. Within the solid, changes must occur prior to failure. Ultimate failure is perhaps best described as the final unstable manifestation of these changes. An example is the phenomenon of dilatancy.[19] Aside from increasing the generality of the code's constitutive relations, the successful modeling of such prefailure mechanisms could help to avoid the problem of treating failure as a discontinuous process. Thus, the numerical as well as the physical model might be improved.

Melting—The phenomenon of melting is treated very simply by SOC within the same routine as the constitutive relations for a solid. Melting and subsequent unloading are assumed adiabatic. At each cycle, the internal energy E (per unit volume) of each zone is compared with the melt energy E_f as specified by the user. If $E > E_f$, then the shear modulus and shear stress are set to zero but the zone retains knowledge of prior cracks, if any, although ductility usually eliminates them. The P-mu curve remains the same as for the solid. If the internal energy drops below the melt energy upon unloading, the zone returns to the solid state. Note that the user must specify some kind of failure preferably ductile, to occur prior to melting, lest the material retain a finite shear stress which is suddenly zeroed.

More precise models of melting behavior in rock materials than the above have not yet been developed. The concept of melting used by SOC has been developed following the reasoning of Butkovich.[20] When a volume of material is compressed and distorted by a shock wave, and then subsequently unloads, the work done by the shock loading is not entirely returned to the motion of the material. If this left-over or "waste" energy is assumed to be in the form of heat, and it is sufficiently large, then, according to SOC, it will cause melting. (One can, however, imagine that some of the energy may remain instead as permanent distortion, or as the heat necessary for a solid-solid phase transition, chemical reaction, etc.) Furthermore, if it is assumed that the shock loading and subsequent unloading curve for a given material are always approximately the same, then the critical amount

of "waste heat" for melting may be related to the internal energy. The melt energy E_f is somewhat arbitrarily chosen to be about one half that for vaporization. (See the next section for further explanation.)

Constitutive Relations for a Gas

Vaporized material has no strength in shear, hence no deviatoric stress may exist. We therefore need only investigate the pressure-density relationship. However, since we consider the expansion (or compression) of a material containing a considerable amount of heat, we need a relationship of the form $P = P(\rho, E)$. First, we must decide upon the criterion for vaporization.

The concept of using the internal energy in a zone as an indicator for vaporization[20] is basically the same as has been described in the previous section for melting. In fact, the concept was developed for a gas and then applied to melting. The same limitations still apply. Basically, the user specifies a vaporization energy E_v which is the internal energy (per unit volume) necessary for complete vaporization. Partially vaporized states are not considered. The value of E_v is at best an educated guess. Butkovich[18] assumes that the "waste heat" necessary to vaporize SiO_2 (the major constituent of most rocks) is 2800 cal/g. If one combines this number with a loading Hugoniot (also assumed to be the unloading curve) for the solid rock material of interest, he can arrive at the vaporization pressure for that material. An example is given in Fig. 15. This method, though highly approximate, is probably as good as our current

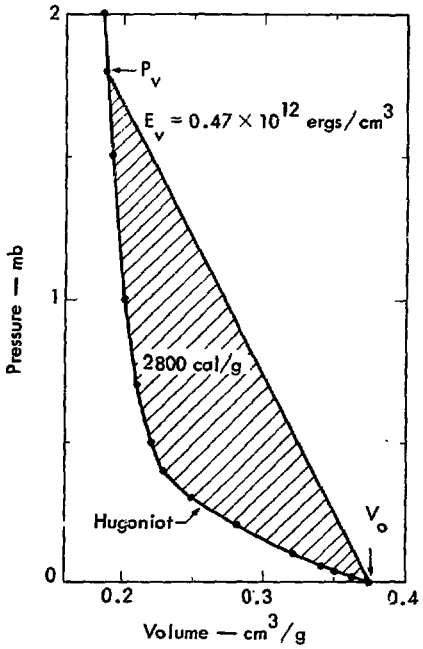

Fig. 15. Shock Hugoniot for granite showing how energy and pressure of vaporization are obtained.[20] P_v and E_v are determined from $E_v = 1/2\ P_v\ \Delta V/V_o$ when the shaded area is 2800 cal/g.

understanding of the shock vaporization process. Continued loading above the vaporization pressure follows the initial P-mu loading curve. The only problem then is to define the adiabatic unloading curve that the gas follows when it expands.

Butkovich expresses the gas equation of state, which determines the expansion as

$$\gamma - 1 = \frac{PV}{E}, \tag{38}$$

where γ is the effective isentropic or adiabatic exponent. In essence, he treats the gas as an ideal gas for each small

change in unloading state (the equivalent of incremental elasticity) and calculates the necessary tables. The user has three options. The first two are to provide a table of values of P, E, and ρ or a table of $(\gamma - 1)$, E, and ρ. In either case, since the code at any point has calculated E and ρ, the use of the table and Eq. (38) will yield the pressure. Butkovich[20] and Rodean[21] discuss the aptness of the approximations that are involved. The reason for the two-table redundant option is that $(\gamma - 1)$ varies over a much smaller range than P, and the resulting numbers are easier to manipulate. The third option is simply to specify a "short gas table" consisting of one set of P and V values for unloading from the initial density ρ_0. The validity of the use of the short table depends mostly on the assumption that all of the vaporized material unloads from a single P-V state at vaporization. This is probably sufficiently accurate for most purposes, but it is seldom necessary to use a short table in view of the availability of the complete tables and fast computers. A sample P, E, ρ table is shown graphically in Fig. 16.

Constitutive Relation for a State of "Water Release"

In a rock material which contains water, there is a possible state which is not accounted for by the constitutive relations thus far described, that is, when the rock material is solid or liquid, but the water has been vaporized. The adiabatic unloading of such a two-phase system has been calculated by Butkovich.[22]

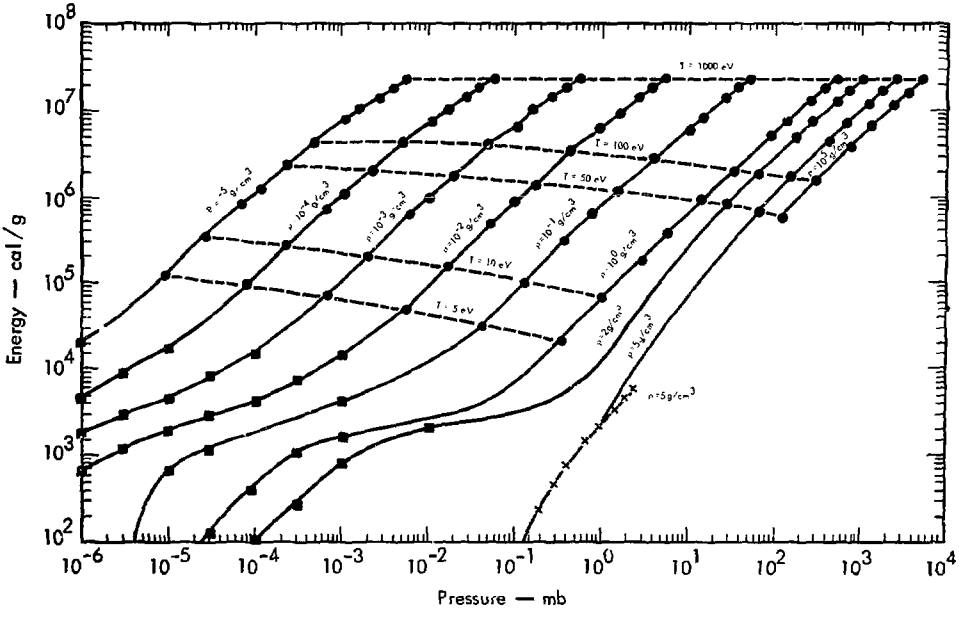

Fig. 16. Equilibrium equation of state for SiO_2 and 1% H_2O by weight.[20]

Basically, he combines, by volume weighting, the unloading curves for the solid with the unloading adiabat for water to obtain an unloading curve for the system.

In SOC, the P-V adiabatic release curves for water are stored in the code, and the user need only specify the weight fraction of water and a total volumetric strain above which all of the water is assumed to vaporize. For continued loading, the material follows the input P-mu curve, but for unloading, the appropriate expansion adiabat is followed (Fig. 17). Butkovich has determined that a mu corresponding to a pressure of

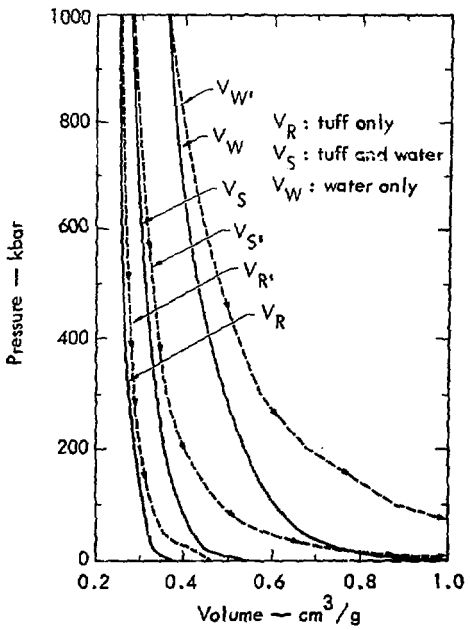

Fig. 17. Loading and release paths for Schooner tuff, water, and tuff-water combination.[20] Dashed curves, identified by primed letters, are for release from 1 mb.

100 kbar is a sufficiently good approximation for satisfactory results. Of course, in the actual case, there is a minimum pressure for the onset of vaporization (about 50 kbar) and a maximum pressure for total vaporization (about 700 kbar), and in between, there exists a solid-liquid-gas system. However, in light of current computational accuracies, it is not necessary to calculate the complete system. The use of a single mu to characterize water vaporization is sufficient.

Constitutive Relations for a High Explosive

Due to the finite velocity of detonation, and the complex thermodynamic nature of the expanding gases produced by a high explosive (HE), SOC treats HE in a separate routine. Basically, one determines from the detonation velocity and properties of the explosive (as provided by the user) whether or not burn has occurred in the zone. If burn has occurred, the subsequent adiabatic expansion is determined from a set of tables developed by Lee, et al.[23] It does not appear at this point that there are any severe problems with the SOC formulation.

ENERGY

The internal energy of a zone is used explicitly for the determination of the shear modulus weighting factor (wt), the melting point, the vaporization point, and, if the material is vaporized, the point it occupies on the gas tables. Other than these applications, the remaining purpose of the energy calculation is as a consistency

check. Because the adiabatic process that we consider can only transfer energy mechanically, the total mechanical energy (internal plus kinetic) of all the zones must remain equal to whatever energy is given as input to the problem. To calculate the total energy, we note that the time rate of change of the internal (strain) energy of a zone is given by

$$\dot{E} = \sigma_{rr}\dot{\epsilon}_{rr} + 2\sigma_{\theta\theta}\dot{\epsilon}_{\theta\theta} . \qquad (39)$$

To put this in the form that SOC uses, we combine Eqs. (4), (5), and (14) to obtain

$$\dot{E} = -\frac{P\dot{V}}{V} - \frac{2}{3}K\left(-\frac{\dot{V}}{V} + 3\frac{\partial U_r}{\partial r}\right) . \qquad (40)$$

Equation (40) is used to find the change in internal energy after each time step. To this, we add the kinetic energy, and then sum over all the zones to find the total energy. (We may also add the gravitational potential energy, if necessary.) When a problem is terminated, any discrepancy between the accumulated energy of all the zones and the energy provided by input may be attributed to numerical error.

This section completes the description of a SOC calculation for one time increment Δt. The next step is to return to the equation of motion and, using the newly-calculated stress state, to begin the loop again. This process is continued until a sufficient time segment, as determined by the user, has elapsed.

INITIATION OF A SOC PROBLEM

This report is not meant to be a user's manual. Nevertheless, it would be worthwhile to describe several of the means of energizing the medium (which in turn cause the motion).

Complete Simulated Nuclear Explosive

The simulation of a nuclear explosion with SOC is achieved as follows: The inner most region in the problem is specified as "iron gas" with the appropriate volume and mass of the nuclear device (made to be spherical). This volume of gas is given an initial internal energy equal to the yield of the device. The subsequent cavity expansion, vaporization of rock material, and motion are then calculated by the code.

"Bubble" Simulated Nuclear Explosive

The so-called "bubble" was developed as a means of approximating the complete problem as described above, but with the use of less computer time. Currently, there is seldom need for the small time savings, but the bubble still may be a convenience for some. The bubble assumes that 70 metric tons of rock are vaporized per kiloton of device yield.[18] The problem starts with a vaporized volume of rock gas at exactly the radius beyond which no more vaporization occurs. This volume contains the energy of the device distributed uniformly. No iron gas is considered, because the volume of the rock gas bubble is considerably larger than the volume of the iron in the device. The bubble is obviously a fairly crude approximation to a true device for early times or close to the expanding cavity. However, it has proved to be quite adequate at later times and farther from the source.

Chemical High Explosive

A volume of HE material may be the SOC source of energy. In this case the HE may be placed anywhere and allowed to yield energy in some finite time (as compared to a nuclear explosion, which is essentially instantaneous).

Pressure at a Boundary

If one calculates the pressure versus time at a nuclear-caused cavity wall, he sees an initial peak followed by a more-or-less exponential decay (possibly with some ringing). It is a sufficient approximation for many problems, and certainly allows savings of computer time and unnecessary complexity, to simply use pressure as a function of time at an internal boundary to initiate motion. This is often a good way to perform parameter studies, since problems such as cavity ringing are avoided.

Velocity in a Region

There are some problems, such as projectile impact, which require a mass with a prescribed velocity to initiate the motion of a medium. SOC allows this option, although it does not ordinarily apply to explosion problems.

SAMPLE SOC PROBLEMS

This section contains the results of four representative SOC calculations. All four calculations use a 1 kt "bubble" energy source. The initial cavity radius and pressure are 1.86 m and 1.72 mb respectively. The first calculation is for an essentially linearly elastic material (no failure and constant bulk and shear moduli). The second calculation introduces a very simple failure surface and more realistic bulk modulus versus pressure relationship, although a simplified stress relaxation scheme is used. The third calculation introduces a more realistic failure surface, and the fourth calculation uses the complete SOC stress relaxation scheme.

The purpose of these sample calculations is to show that, although SOC works acceptably well for the elastic case, the successive introduction of several non-elastic phenomena produces increasingly questionable results. We have purposely chosen calculations that emphasize SOC's difficulties. If we had used a larger energy input, or weaker material, many of these difficulties would not have arisen.

Elastic

Material properties for the elastic case are given in Table 1. We show, in Fig. 18, velocity (V), pressure (P), and shear stress (K) versus radius at time t = 5 msec after problem initiation. Figures 19 and 20 show P and K versus time at, respectively, the cavity radius and at the zone with an initial radius of 6.41 m. The results shown are quite straightforward and acceptable. The noise indicated is a result of some "ringing" in the cavity and numerical instability. We show all of these figures so that they may be compared with the subsequent non-elastic results.

Table 1. Material properties for elastic case.

Property	Value
Initial density	2.61 g/cm^3
Bulk modulus	0.33 mb
Rigidity modulus	0.200 mb

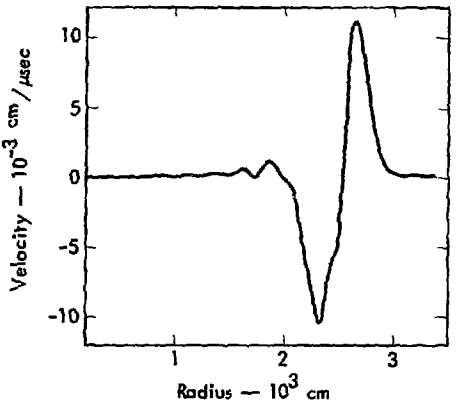

Fig. 18a. Elastic sample problem showing velocity at 5 msec.

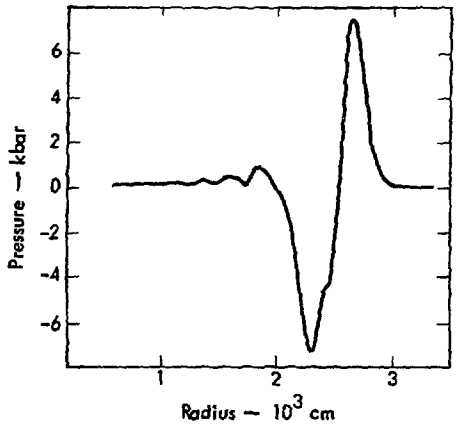

Fig. 18b. Elastic sample problem showing pressure at 5 msec.

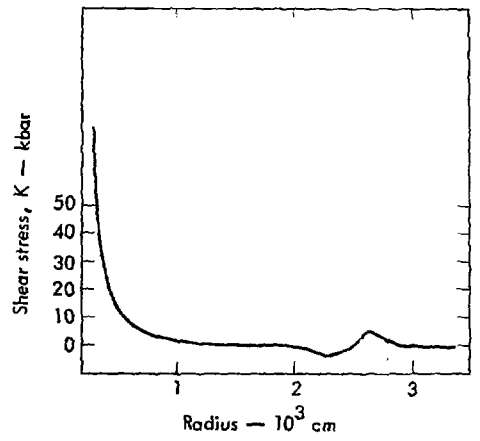

Fig. 18c. Elastic sample problem showing shear stress at 5 msec.

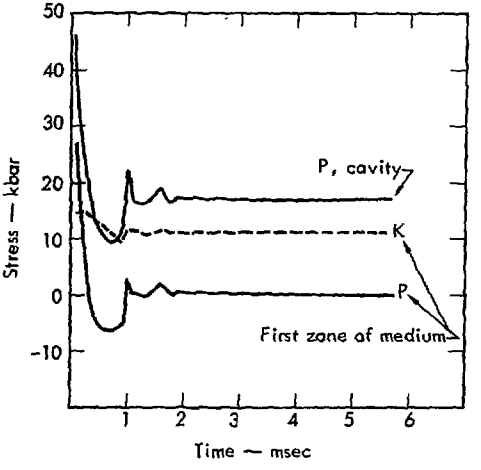

Fig. 19. Elastic sample problem. P and |K| versus time at the cavity radius.

Simple Failure

The material properties used for this sample problem are given in Table 2 and Fig. 21. The failure surface, $|K|$ versus $\bar{P}$, in this material is simply a constant, as for an elastic-plastic material, except that both brittle and ductile failure are allowed. The stress relaxation scheme, however, differs from the SOC model in that the viscosity term in Eq. (29) has

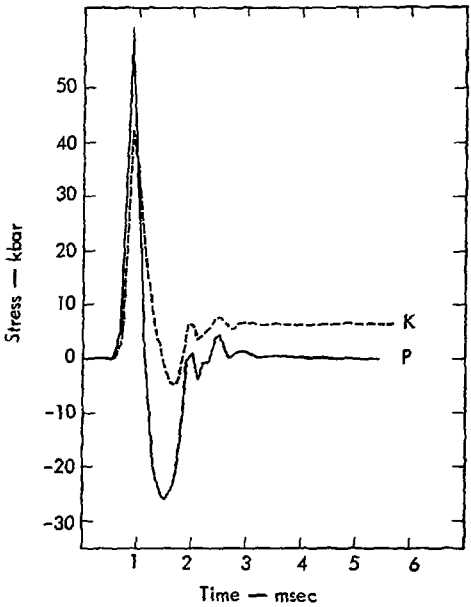

Fig. 20. Elastic sample problem. P and |K| versus time at the zone with an initial radius of 6.41 m.

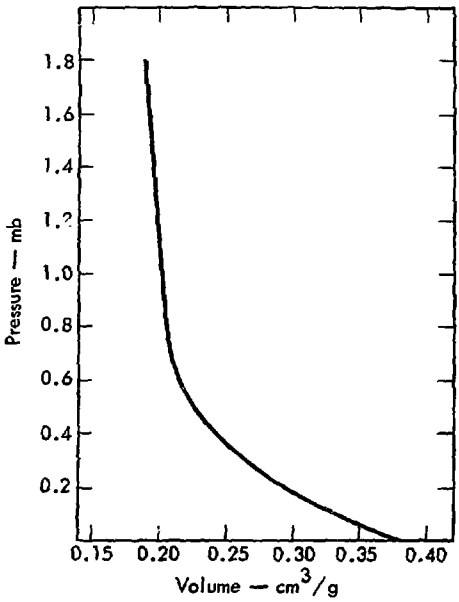

Fig. 21. Pressure-volume relationship for non-elastic sample problems.

Table 2. Material properties for simple failure sample problem.

Property	Value
Initial density	2.61 g/cm^3
Pressure-volume relation	See Fig. 21
Poisson's ratio	0.25
Failure stress	15 kbar
Brittle-ductile transition	0.065 mb
"Bulking" strain	-0.14

been replaced by μ/η = 0.001/sec. This has been done to simplify the relaxation scheme such that the gross features of failure as described by SOC can be emphasized. Normally, SOC relaxation begins slowly, but finishes very rapidly, while the scheme in this example produces a constant relaxation rate.

Figure 22 shows V, P, and K versus radius at t = 5 msec. Due to the SOC treatment of failure, several discontinuities and considerable noise have appeared. These are particularly noticeable in the P and K plots. To see why these arise, we have plotted P and K versus time for three pairs of adjoining zones that find themselves in the situations shown in Figs. 23a, 24a, and 25a. The first pair of zones, at 6.3 m, is one that sees both ductile and brittle failure and one that sees only ductile failure. The second pair of zones, at 7.8 m, is a zone that sees ductile failure

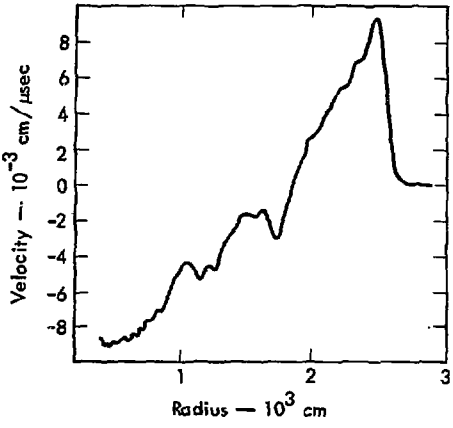

Fig. 22a. Sample problem with simple failure, showing velocity at 5 msec.

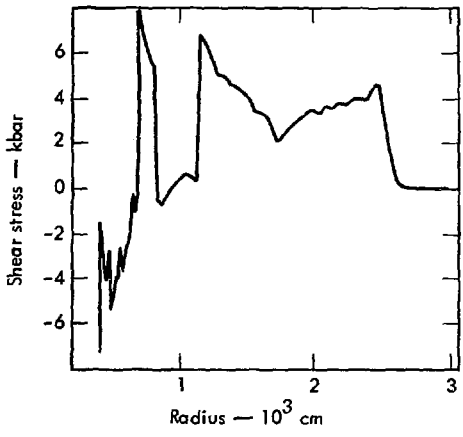

Fig. 22c. Sample problem with simple failure, showing shear stress at 5 msec.

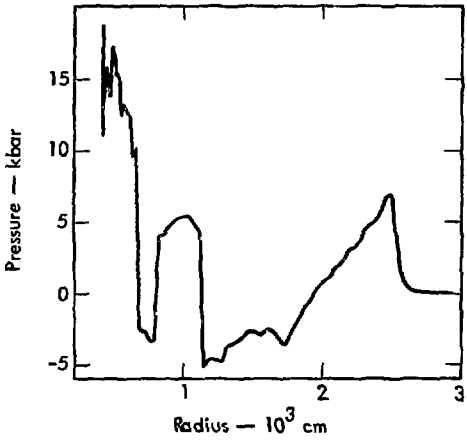

Fig. 22b. Sample problem with simple failure, showing pressure at 5 msec.

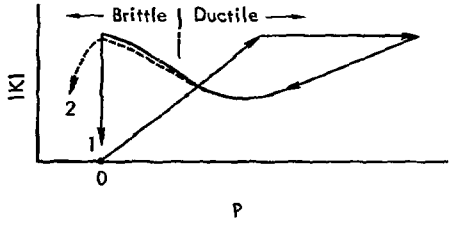

Fig. 23a. Sample problem with simple failure, showing schematic stresspaths for a pair of adjoining zones at 6.3 m. Both start at 0,0. Zone 1 fails ductile and then brittle, while Zone 2 fails ductile only.

only and one that sees brittle failure only. The third pair of zones, at 11.2 m, is a zone of brittle failure and an adjoining elastic zone.

The time plots in Figs. 23b, 24b, and 25b contain discontinuities which result from the zeroing of P and K depending upon the stress histories of the zones. These discontinuities act effectively as internal boundaries in the problem and produce reflections, dispersions, etc.,

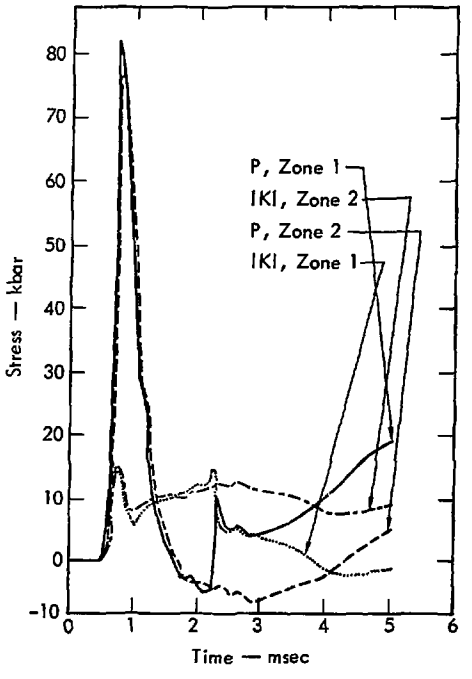

Fig. 23b. Sample problem with simple failure, showing pressure and $|\bar{K}|$ versus time for the zones of Fig. 23a. A stress discontinuity arises at $\bar{P} = 0$ when Zone 1 suddenly goes to "special loading."

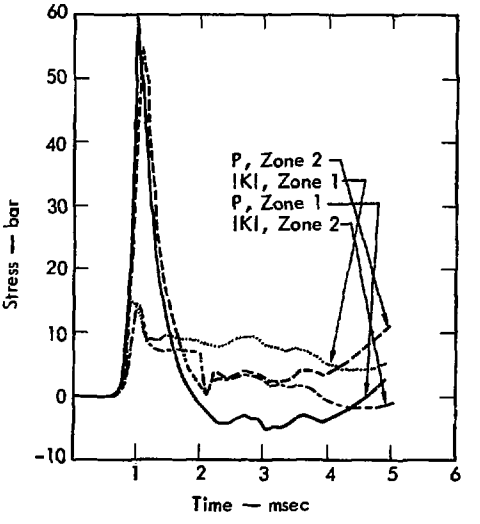

Fig. 24b. Sample problem with simple failure, showing pressure and $|\bar{K}|$ versus time for the zones of Fig. 24a. A stress discontinuity arises at $\bar{P} = 0$ when Zone 2 goes to "special loading."

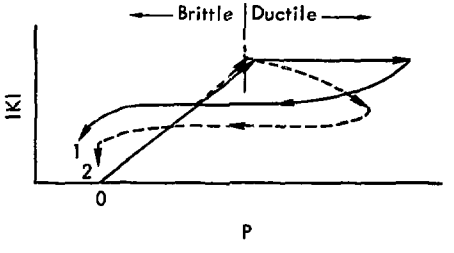

Fig. 24a. Sample problem with simple failure, showing schematic stress paths for a pair of adjoining zones at 7.8 m. Both start at 0,0. Zone 1 fails ductile only. Zone 2 fails brittle only.

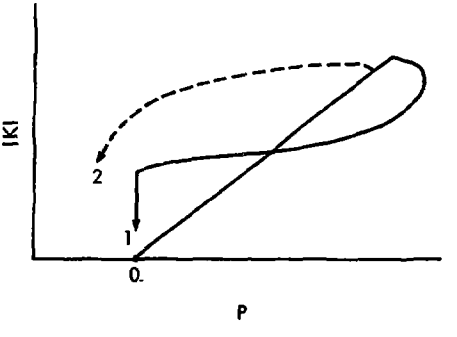

Fig. 25a. Sample problem with simple failure, showing schematic stress paths for a pair of adjoining zones at 11.2 m. Both start at 0,0. Zone 1 fails brittle. Zone 2 does not fail.

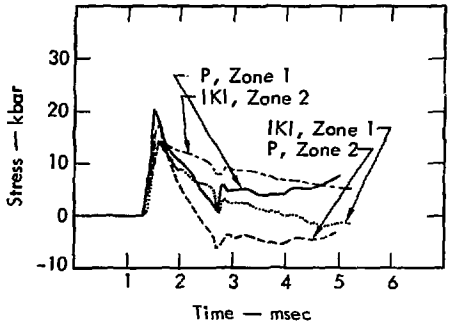

Fig. 25b. Sample problem with simple failure, showing pressure and $|\bar{K}|$ versus time for the zones of Fig. 25a. A stress discontinuity arises at $\bar{P} = 0$ when Zone 1 goes to "special loading."

as would any boundary. They are, however, not representative of real-world boundaries. In a single body of rock, the stress-strain-failure relations should not in general be entirely different for an infinitesimal change in position. To be sure, a boundary between pure materials, or between individual grains in a rock, may act this way, but the average properties of bulk rock should be more continuous. A zone in SOC, which represents an entire spherical shell many cubic meters in volume, should not suddenly be all brittle and then all ductile. This discontinuities which arise in this example indicate a real deficiency in the SOC code, even in cases where the overall aspects of the motion as calculated may be accurate.

More Realistic Failure

The material properties are given in Table 3 and Fig. 26. The only essential difference between this and the previous sample problem is the decrease of the

Table 3. Materials for a more realistic failure sample problem.

Property	Value
Initial density	2.61 g/cm^3
Pressure-volume relation	See Fig. 21
Poisson's ratio	0.25
Failure strength	See Fig. 26
Brittle-ductile transition	0.065 mb
"Bulking" strain	-0.14

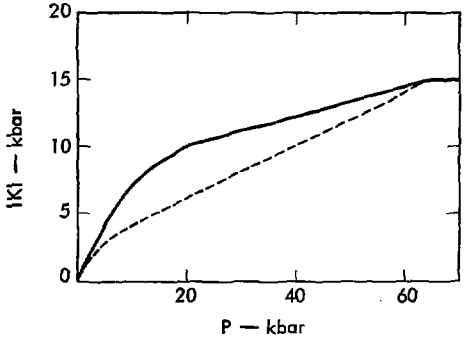

Fig. 26. Failure surfaces in $|\bar{K}|$-$\bar{P}$ space for sample problem with more realistic failure. Solid line is loading (initial failure) curve and dashed line is unloading (subsequent failure) curve.

failure surface toward zero for tension. V, P, and K versus radius at 5 msec are shown in Fig. 27. Similar features appear as in the previous example, except that they are somewhat obscured by the decreased strength near to $\bar{P} = 0$.

Complete SOC Failure Model

The example is exactly the same as the above except that the SOC "cracking" scheme is used. V, P, and K versus radius at 5 msec are shown in Fig. 28.

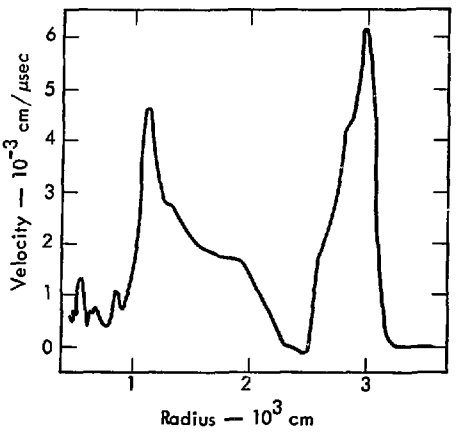

Fig. 27a. Sample problem with more realistic failure, showing velocity at 5 msec.

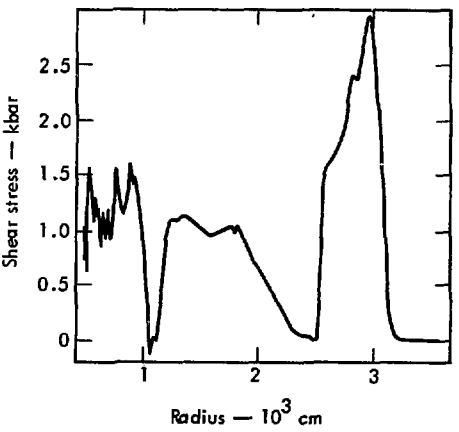

Fig. 27c. Sample problem with more realistic failure, showing shear stress at 5 msec.

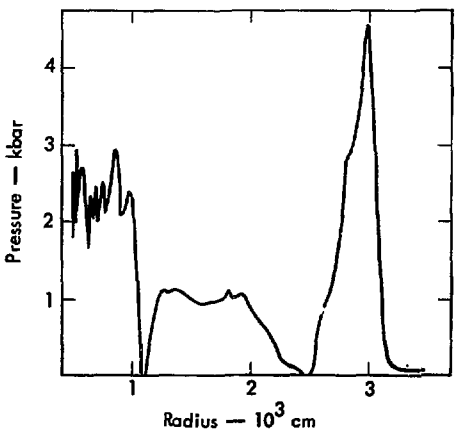

Fig. 27b. Sample problem with more realistic failure, showing pressure at 5 msec.

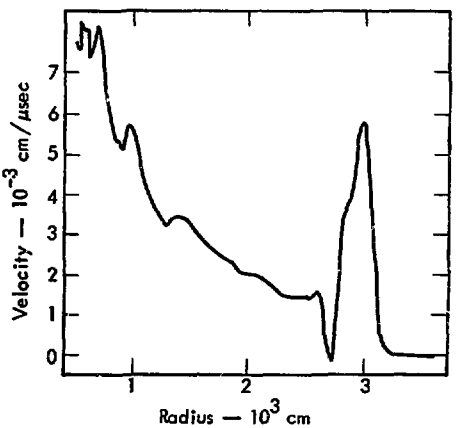

Fig. 28a. Sample problem with SOC failure model, showing velocity at 5 msec.

The increased noise as compared with the previous sample calculations is due to the SOC relaxation scheme, which begins slowly, but becomes very violent before cracking ceases.

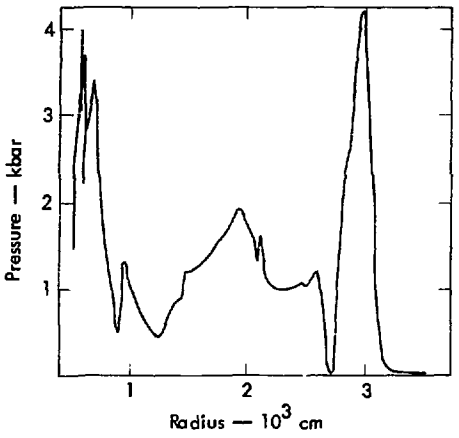

Fig. 28b. Sample problem with SOC failure model, showing pressure at 5 msec.

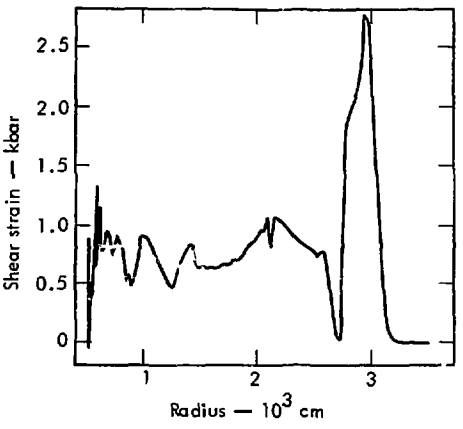

Fig. 28c. Sample problem with complete SOC failure model, showing shear stress at 5 msec.

TENSOR Physics*

Insofar as physics is concerned, the main differences between SOC (the one dimensional code) and TENSOR (the two dimensional code) are found in their constitutive relation formations. These differences are the result of the generalizations necessary to describe the additional dimension in TENSOR. In most cases, the generalized quantities are invarient, independent of zone size, and reduce to the quantities found in SOC for a one dimensional problem. An exception is the case of stress relaxation following brittle failure in which the dependence of the existing unsatisfactory scheme on the zone length in one dimension and on an "average" length in two dimensions may cause the relaxation to differ in the two codes (although intent of the formulation is the same). A discussion of the various quantities of interest follows.

In TENSOR, the relevant physical components of stress, deviators, and mean stress which are appropriate for a cylindrical coordinate system, r, z, ϕ, with axial symmetry, are defined by Cherry et al.[4]

Stresses: T_{rr}, T_{zz}, $T_{\phi\phi}$, T_{rz}.

Pressure: $P = -\frac{1}{3}(T_{rr} + T_{\phi\phi} + T_{zz})$.

Stress deviators:

$$T_r = P + T_{rr},$$
$$T_z = P + T_{zz},$$
$$T_\phi = -(T_r + T_z). \qquad (41)$$

*This section contributed by W. J. Hannon.

As a generalization of the quantity K used in SOC Eq. (2), TENSOR uses the invariant quantity

$$Y = (3/4\ I_{2D})^{1/2} , \qquad (42)$$

where

I_{2D} is the second deviatoric invariant[24] given by

$$I_{2D} = \frac{1}{6}\left[(T'_{11} - T'_{22})^2 + (T'_{22} - T'_{33})^2 + (T'_{33} - T'_{11})^2\right] + T'^2_{12} + T'^2_{13} + T'^2_{32} , \qquad (43)$$

where

$T'_{ij} = P\delta_{ij} + T_{ij}$ = stress deviators,

T_{ij} = physical components of the stress tensor (orthogonal basis), and

δ_{ij} = Kronecker delta.

To write Eqs. (42) and (43) in two dimensions using the notation of Eq. (41), note that

$$T'_{11} = T_r,\ T'_{22} = T_z,\ T'_{12} = T_{rz},\ T'_{33} = -(T_r + T_z)$$

$$T'_{23} = T'_{13} = 0 . \qquad (44)$$

These substitutions give

$$I_{2D} = T_r^2 + T_z^2 + T_r T_z + T_{rz}^2 , \qquad (45)$$

and

$$Y = \left[3/4\left(T_r^2 + T_z^2 + T_r T_z + T_{rz}^2\right)\right]^{1/2} . \qquad (46)$$

In the case of one dimension, for both spherical and plane problems,

$$T'_{11} = P + \sigma_{rr},\ T'_{22} = T'_{33} = P + \sigma_{\theta\theta} ,$$

$$T'_{12} = T'_{13} = T'_{23} = 0 , \qquad (47)$$

where σ_{rr} and $\sigma_{\theta\theta}$ are defined in Eqs. (4) and (5).

This gives

$$I_{2D} = \frac{1}{3}(\sigma_{rr} - \sigma_{\theta\theta})^2 , \qquad (48)$$

and

$$Y = |K| . \qquad (49)$$

Although it can be shown that in the spherical and plane SOC geometries K is proportional to the maximum shear stress, the octahedral shear stress, and the square root of the strain energy of distortion, Y, in general, is proportional only to the last two. Thus, Y cannot be considered to be a generalization of a failure criterion based on maximum shear stress. It is interesting to note that in the case of one dimensional symmetry (i.e., dependence only on the distance from the z axis) we can no longer make the assumption that the azimuthal stress, $\sigma_{\phi\phi}$, equals the axial stress, σ_{zz}. Instead, the axial stress is determined from the condition that the axial strain e_{zz} is zero. We find that $\sigma_{zz} = \nu(\sigma_{rr} + \sigma_{\phi\phi})$, where ν is Poisson's ratio. Thus, in general, σ_{zz} does not equal either of the other two principal stresses and may be such that the differences given by $|\sigma_{zz} - \sigma_{rr}|$ or $|\sigma_{zz} - \sigma_{\phi\phi}|$ may be larger than $|\sigma_{rr} - \sigma_{\phi\phi}|$. Under these conditions the use of K is probably an inadequate failure criterion and Y should be used even in the one dimensional code.

Although Y can be looked upon as a generalized expression consistent with a failure criterion based on distortional

strain energy or octahedral shear stress, the generalized form of $\bar{P}$ does not appear to have such a specific physical interpretation. An invariant form in two and three dimensions which reduces to $\bar{P} = P + K/3$ in the usual SOC cases is

$$P = \frac{I_1}{3} - \frac{1}{2}\left(\frac{1}{2} I_{3D}\right)^{1/3} , \qquad (50)$$

where

I_1 = the first stress invariant,

I_{3D} = the third deviatoric stress invariant

= det (T'_{ij}) .

In practice, a Y-$\bar{P}$ criterion provides a convenient way of using a single failure criterion for a variety of stress states. (See the previous discussion for SOC.) It does not represent a fundamental physical relationship and should be used with caution.

As in the case of SOC, TENSOR makes a distinction between shear failure and tension failure. This distinction is made on the basis of the algebraically largest principal stress. The principal deviatoric stresses, S_i, are given by

$$S_1 = -(T_r + T_z) ,$$

$$S_{2,3} = \frac{1}{2}\left\{(T_r + T_z) \pm \left[(T_r - T_z)^2 + 4T_{rz}^2\right]^{1/2}\right\} . \qquad (51)$$

This is easily seen by noting that one of the principal deviatoric stresses is T_ϕ, and that the other two are equivalent to a state of plane stress in the r, z, plane.[24] The principal stresses are formed in the usual way. If the largest principal stress is greater than zero and the failure surface is exceeded, then the material is assumed to fail in tension. The "crack velocity" is adjusted as described in the SOC section. No provision is made for an anisotropic change in material properties due to the failure.

In the event that brittle failure has occurred, stress relaxation takes place. The relaxation scheme is essentially that given in the SOC description. A complication occurs in the two dimensional code because of the necessity of defining a linear zone dimension, DL, with which the "crack length" can be compared. This zone dimension is determined by letting $\underline{D}_1$ and $\underline{D}_2$ be the vectors corresponding to the diagonals of the zone. We then define a variable, L_D, where

$$L_D = \frac{1}{2} \max \left\{\left|\underline{D}_1 + \underline{D}_2\right|, \left|\underline{D}_1 - \underline{D}_2\right|\right\} . \qquad (52)$$

If the zone were a rectangle, L_D would correspond to the length of the longest side. The zone dimension, DL, is then defined as the area divided by L_D. Relaxation proceeds as in SOC using the value of DL in place of ΔR in Eq. (29). In comparing SOC and TENSOR calculations it is important to note that the TENSOR zoning can cause DL to differ from ΔR, even for spherical zoning with the same radial spacing of zones. This will cause the effective relaxation schemes to differ in the two codes.[25]

The above comments point out the major differences in the formulations of constitutive relations for solids in SOC and TENSOR. In addition to these differences, others exist in the areas of the other constitutive relations and the treatment of artificial viscosity. In

particular, TENSOR does not have the extended gas tables in the form of Eq. (38). A gas table giving pressure versus radius may be entered for a spherical source region, and a table giving pressure versus mu corresponding to the short table of SOC may be entered. Also, there is no provision at all for water release (at present). In those relatively simple cases for which the same problem can be run on both SOC and TENSOR, the differences in the calculated velocities, displacements, and stresses are less than a few percent.[26]

Conclusions

To become truly viable predictive tools, particularly in the case of a medium for which there is little or no prior experience, SOC and TENSOR need considerable revision. The major physics-associated effort of such revision should be in the formulation and use of constitutive relations for solid materials. (There are, of course, many strictly numerical improvements which are also necessary.) Such a revision of SOC has already been undertaken, and the resulting code named SOC73, is essentially completed and will be described in a subsequent report. An improved, but as yet unnamed, two-dimensional code is also being developed.

References

1. F. C. P. Seidl, "SOC," A Numerical Model for the Behavior of Materials Exposed to Intense Impulsive Stresses, Lawrence Livermore Laboratory, Rept. UCID-5033 (1965).
2. J. T. Cherry and F. L. Petersen, Numerical Simulation of Stress Wave Propagation from Underground Nuclear Explosions, Lawrence Livermore Laboratory, Rept. UCRL-72216 (1970).
3. G. Maenchen and S. Sack, "The Tensor Code," Methods in Computational Physics, B. Alder, Ed. (Academic Press, New York, 1964), Vol. 3, pp. 181-210.
4. J. T. Cherry, S. Sack, G. Maenchen, and V. Kransky, Two-Dimensional Stress-Induced Adiabatic Flow, Lawrence Livermore Laboratory, Rept. UCRL-50987 (1970).
5. J. Von Neumann and R. D. Richtmyer, "A Method for the Numerical Calculation of Hydrodynamic Shocks," J. Appl. Phys. 21, 232 (1950).
6. I. Y. Borg, Survey of Piledriver Results and Preliminary Interpretation of Three Postshot Cores In and Near the Cavity, Lawrence Livermore Laboratory, Rept. UCRL-50865 (1970).
7. R. D. Richtmyer and K. W. Morton, Difference Methods for Initial Value Problems, (Interscience, New York, 1967) 2nd ed.
8. J. C. Jaeger and N. G. W. Cook, Fundamentals of Rock Mechanics (Chapman and Hall, Ltd., 1971).
9. R. Aris, Vectors, Tensors, and the Basic Equations of Fluid Mechanics (Prentice-Hall, Englewood Cliffs, NJ, 1962), pp. 190-192.
10. R. N. Schock, H. C. Heard, and D. R. Stephens, Stress-Strain Behavior of a Granodiorite and Two Graywackes on Compression to 20 Kilobars, Lawrence Livermore Laboratory, Rept. UCRL-51261 (1972).
11. K. Mogi, "Effect of the Intermediate Principal Stress on Rock Failure," J. Geophys. Res. 72, 5117 (1967).
12. J. Handin, H. C. Heard, and J. N. Magouirk, "Effects of the Intermediate Principal Stress on the Failure of Limestone, Dolomite, and Glass at Different Temperatures and Strain Rates," J. Geophys. Res. 72, 611-640 (1967).
13. J. White, Lawrence Livermore Laboratory, Internal Document UOPKA 71-8 (1971). Readers outside the Laboratory who desire further information on LLL internal documents should address their inquiries to the Technical Information Department, Lawrence Livermore Laboratory, Livermore, California 94550.
14. J. White, An Invariant Description of Failure for an Isotropic Medium, Lawrence Livermore Laboratory, Rept. UCRL-72065 (1972).
15. M. L. Wilkins, The Calculation of Elastic-Viscous-Plastic Effects in Materials, Lawrence Livermore Laboratory, Rept. UCRL-72639 (1970).

16. R. Chin, Lawrence Livermore Laboratory, private communication (1973).
17. Z. T. Bieniawaski, "Fracture Dynamics of Rocks," Int. J. Fracture Mech. 4, 415 (1968).
18. I. Y. Borg, Lawrence Livermore Laboratory, private communication (1972).
19. W. F. Brace, B. W. Paulding, and C. H. Scholz, "Dilatancy in the Fracture of Crystalline Rocks," J. Geophys. Res. 71, 16 (1966).
20. T. R. Butkovich, The Gas Equation of State on Natural Materials, Lawrence Livermore Laboratory, Rept. UCRL-14729 (1967).
21. H. C. Rodean, Nuclear Explosion Seismology, (U.S. Atomic Energy Commission, Oak Ridge, TN, 1971).
22. T. R. Butkovich, "Influence of Water in Rock on Effects of Underground Nuclear Explosions," J. Geophys. Res. 76, 1993 (1971).
23. E. L. Lee, H. C. Hornig, and J. W. Kury, Adiabatic Expansion of High Explosive Detonation Products, Lawrence Livermore Laboratory, Rept. UCRL-50422 (1968).
24. Y. C. Fung, Foundations of Solid Mechanics (Prentice-Hall, Englewood Cliffs, NJ, 1965) pp. 80-81.
25. J. White, Lawrence Livermore Laboratory, private communication (1973).
26. R. Terhune, Lawrence Livermore Laboratory, private communication (1972).